DOI:
10.1126/science.aad1210

Document Version
Peer reviewed version

Title: Intrinsic NLRP3 inflammasome activity is critical for normal adaptive immunity via regulation of IFN-γ in CD4$^+$ T cells

Authors: Giuseppina Arbore[1,*], Erin E. West[2,*], Rosanne Spolski[2], Avril A. B. Robertson[3], Andreas Klos[4], Claudia Rheinheimer[4], Pavel Dutow[4], Trent M. Woodruff[3], Zu Xi Yu[5], Luke A. O'Neill[6], Rebecca C. Coll[3], Alan Sher[7], Warren J. Leonard[2], Jörg Köhl[8,9], Pete Monk[10], Matthew A. Cooper[3], Matthew Arno[11], Behdad Afzali[1,12], Helen J. Lachmann[13], Andrew P. Cope[14], Katrin D. Mayer-Barber[15], Claudia Kemper[1,2,**]

Affiliations:

[1]MRC Centre for Transplantation, Division of Transplant Immunology and Mucosal Biology, King's College London, London SE1 9RT, United Kingdom.

[2]Laboratory of Molecular Immunology and the Immunology Center, National Heart, Lung, and Blood Institute (NHLBI), National Institutes of Health (NIH), Bethesda, MD 20892-1674, USA.

[3]Institute for Molecular Bioscience and School of Biomedical Sciences, University of Queensland, Queensland QLD 4072, Australia.

[4]Institute for Medical Microbiology and Hospital Epidemiology, Medizinische Hochschule Hannover, Hannover 30625, Germany.

[5]Pathology Core, National Heart, Lung, and Blood Institute (NHLBI), National Institutes of Health (NIH), Bethesda, MD 20892, USA.

[6]School of Biochemistry and Immunology, Trinity College Dublin, Dublin, Ireland.

[7]Laboratory of Parasitic Diseases, National Institute of Allergy and Infectious Diseases (NIAID), NIH, Bethesda, MD 20892, USA.

[8]Institute for Systemic Inflammation Research, University of Lübeck, Lübeck, Germany.

[9]Division of Immunobiology, Cincinnati Children's Hospital Medical Center and University of Cincinnati College of Medicine, Cincinnati, OH, USA.

[10]Department of Infection and Immunity, University of Sheffield, Sheffield S10 2RX, United Kingdom.

[11]Genomics Centre, Faculty of Life Sciences and Medicine, King's College London, London SE1 9NH, United Kingdom.

[12]Lymphocyte Cell Biology Section, Molecular Immunology and Inflammation Branch, National Institutes of Arthritis, and Musculoskeletal and Skin Diseases, NIH, Bethesda, MD 20892, USA.

[13]UK National Amyloidosis Centre, Division of Medicine, University College London, Royal Free Campus, London NW3 2PF, United Kingdom.

[14]Academic Department of Rheumatology, Division of Immunology, Infection and Inflammatory Diseases (DIIID), King's College London, London SE1 1UL, United Kingdom.

[15]Laboratory of Clinical Infectious Diseases, Inflammation & Innate Immunity Unit, NIAID, NIH, Bethesda, MD 20892, USA.

*These authors contributed equally to the work; **Correspondence to: claudia.kemper@kcl.ac.uk

Abstract: The NLRP3 inflammasome controls IL-1β maturation in antigen presenting cells but a direct role for NLRP3 in human adaptive immune cells has not been described. Here we show that the NLRP3 inflammasome assembles in human $CD4^+$ T cells and initiates caspase-1-dependent IL-1β secretion, thereby promoting IFN-γ production and Th1 differentiation in an autocrine fashion. Importantly, NLRP3 assembly requires intracellular C5 activation and stimulation of C5a receptor 1 (C5aR1), which is controlled by surface-expressed C5aR2. Dysregulation of NLRP3 activity in T cells affects inflammatory responses in autoimmune disease and infection. First, $CD4^+$ T cells from patients with cryopyrin-associated periodic syndromes (CAPS), who have constitutively-active NLRP3, exhibit overactive Th1 responses that are normalized by NLRP3 inhibitor treatment. Second, IFN-γ production is impaired in T cells from *Nlpr3*$^{-/-}$ mice upon viral infection and alters disease outcome in a colitis model. Our results demonstrate that NLRP3 inflammasome activity is not confined to 'innate immune cells' but is an integral component of normal adaptive Th1 responses.

One Sentence Summary: Non-canonical complement activation in T cells regulates intrinsic NLRP3 inflammasome activity and IFN-γ production.

Main Text: The complement system is an ancient innate immune sensor system and essential for the elimination of pathogens by the host. Processing in serum of liver-derived C3 into C3a and C3b and of C5 into C5a and C5b activation fragments leads to opsonization and removal of invading microbes, mobilization of innate immune cells, and induction of inflammatory reactions (*1*). However, complement also profoundly regulates adaptive immunity: in addition to T cell receptor (TCR) activation, co-stimulation and the presence of interleukin (IL)-12 (*2*), human $CD4^+$ T cells also depend on activation of T cell-expressed complement receptors for normal Th1 induction (*3*). In particular, C3a and C3b are generated intracellularly via cathepsin L-mediated cleavage of C3 in T cells upon TCR activation (*4*). These engage their respective receptors, the G-protein coupled receptor (GPCR) C3a receptor (C3aR) and the complement regulator CD46 (which binds C3b), and induce autocrine IFN-γ (*5*, *6*). Mechanistically, C3aR- and CD46-mediated signals regulate IL-2R assembly and mTORC1 activation, which is required for the metabolic programming essential for IFN-γ induction (*7*). Accordingly, C3- and CD46-deficient patients suffer from recurrent infections and have severely reduced Th1 responses *in vitro* and *in vivo* (*5*, *8*). Conversely, uncontrolled intracellular C3 activation in T cells contributes to hyperactive Th1 responses observed in autoimmunity (*3*, *4, 9*) that can be normalized pharmacologically by targeting intracellular cathepsin L function (*4*).

Given the critical role of intracellular C3 processing in human Th1 biology and the importance of C5a generation in inflammation, we investigated whether human $CD4^+$ T cells also harbour an 'intracellular C5 activation' system contributing to effector responses. Indeed, human $CD4^+$ T lymphocytes isolated from healthy donors contained intracellular stores of C5, producing low levels of C5a in the resting state. TCR activation and particularly TCR + CD46 co-stimulation increased the amounts of intracellular C5a, and this was associated with the secretion of C5a to the cell surface (Fig. 1A and B). C5a, as well as the C5a 'des-Arginized' form of C5a (C5adesArg) generated by carboxypeptidase processing, can bind two distinct GPCR receptors, C5aR1 (CD88) and C5aR2 (GPR77, C5L2) (*10, 11*). Binding of C5a to C5aR1 preferentially mediates pro-inflammatory responses. The function of C5aR2 varies with cell type, and C5aR2 can act either as a non-signalling decoy receptor antagonizing C5aR1 or as an active transducer of pro- or anti-inflammatory signals (*11-14*). While extra- and intracellular localization of both C5aR1 and C5aR2 on human monocytes has been reported (*14*, *15*), expression patterns in human $CD4^+$ T have not been described in detail. Here we show expression of mRNA for both *C5AR1* and *C5AR2* in human $CD4^+$ T cells (Fig. 1C) and protein by immunoblotting (fig. S1A), confocal microscopy (Fig. 1D) and flow cytometry (Fig. 1E and F). While mRNA amounts for *C5aR1* and *C5aR2* varies in T cells (Fig. 1C) (*16*), the protein levels for these receptors are comparable among donors (Fig. 1E). In resting and activated $CD4^+$ T cells, C5aR1 is expressed exclusively intracellularly and in low amounts while the C5aR2 receptor is abundantly present inside and to a lesser degree on the cell surface (Fig. 1F). We corroborated the specificity of reagents used for C5a receptor detection using HEK293 cells that had been stably transfected to express C5aR1, C5aR2 or no receptor (fig. S1B and C) and confirmed the ability of resting and activated human $CD4^+$ T cells to bind C5a based on competitive ^{125}I-C5a binding studies (Fig. 1G and fig. S1D). To determine whether autocrine engagement of the C5a receptors on T cells regulates Th1 induction, we activated human $CD4^+$ T cells with immobilized antibodies to CD3, CD3 and CD28 or CD3 and CD46 in the presence or absence of either a specific antagonist to the C5aR1 (PMX53, *17*), the C5aR1/C5aR2 receptor double antagonist $A8^{\Delta 71\text{-}73}$ (dRA, *18*) targeting only C5aR2 as the C5aR1 is expressed intracellularly, or a specific C5aR2 agonist (*19*). All reagents are cell impermeable. Blocking

C5aR2 activity significantly increased Th1 induction (Fig. 1H, left panel) and activating C5aR2 with the agonist or with C5a or C5adesArg reduced Th1 responses (Fig. 1H, middle panel and fig. S1E). Blockade of the C5aR2 also led to increased Th17 (IL-17) but not Th2 (IL-4) responses (fig. S1F), without altering cell viability (fig. S1G). Consistent with the solely intracellular localization of C5aR1, the C5aR1 specific antagonist had no effect on IFN-γ production (Fig. 1H, right panel). However, reduction of intracellular C5aR1 by siRNA gene targeting led to a commensurate decrease in IFN-γ production (Fig. 1I and fig. S1H). Together, these data show that intracellular C5 activation contributes to induction and control of IFN-γ in $CD4^+$ T cells, via combined activation of the C5aR1 and C5aR2 axes.

To delineate the autocrine C5-driven pathways contributing to regulation of IFN-γ in $CD4^+$ T cells, we performed a transcriptomic analysis using T cells from three healthy donors activated, or not, with anti-CD3 and anti-CD46 in the presence or absence of the C5aR1/C5aR2 antagonist. Surprisingly, we observed enrichment of transcripts associated with inflammasome activation, including *NLRP3* and *IL1B* (Fig. 2A and B and Table S1), in cells activated with anti-CD3 and anti-CD46. Inhibition of C5aR2 further increased some of these transcripts, notably *IL1A* and *IL1B* (fig S2A and Table S2). IL-1α and IL-1β are prototypical pro-inflammatory cytokines, involved in innate immune responses and contributing to the development of several pathogenic autoimmune diseases including type 1 diabetes and arthritis (*20-22*). Both IL-1α and IL-1β bind to the IL-1 receptor 1 (IL-1R1). Antigen-presenting cell (APC)-derived IL-1β supports T cell priming and imprinting of T helper effector function (*23*), including enhancement of IFN-γ and IL-17 production from $CD4^+$ T cells (*24-26*). Further, mice with deletion of the IL-1β signal transducer MyD88 in T lymphocytes cannot generate memory T cells (*27*). Pro-IL-1β is synthesized as a 31 kDa precursor and converted to mature, 17 kDa, IL-1β via caspase-1 cleavage (*28*). Caspase-1 is regulated by proteolytic activation during oligomerization with NLRP3 and the adaptor apoptosis-associated speck-like protein containing a CARD (ASC), which is triggered in response to danger signals (*29-30*). NLRP3 inflammasome function has been described in myeloid innate immune cells, with monocytes as the main source of IL-1β (*25*, *31*), and in several non-immune cell types (such as microglia, endothelial and retinal pigment epithelial cells) (*32-34*); however, canonical NLRP3 inflammasome activity has not been demonstrated in lymphoid adaptive immune cells. We confirmed the presence of an 'NLRP3 signature' in T cells by demonstrating *NLRP3* and *IL1B* gene (fig. S2B) and protein expression, as well as generation of activated caspase-1 and mature IL-1β in activated human $CD4^+$ T cells (Fig. 2C and D and fig. S2C to F). Consistent with our gene array data, anti-CD3 and anti-CD46 activation led to most robust NLRP3 activation and IL-1β generation (Fig. 2D) and increased colocalization of NLRP3 and ASC (Fig. 2E). Notably, both resting naïve and memory $CD4^+$ T cells express NLRP3 protein (fig. S2C and D). Since IL-1β supports Th1 induction (*35*) and is most strongly induced by the Th1-driver CD46, we next assessed whether inhibition of NLRP3 activity in $CD4^+$ T cells perturbs IFN-γ production. To this end, $CD4^+$ T cells were activated in the presence of MCC950, a specific NLRP3 inhibitor (*36*), and Th1, Th2 and Th17 cytokine production measured 36 hours post activation. NLRP3 inhibition during T cell activation specifically attenuated IFN-γ (Fig. 2F), whereas differences in IL-4 and IL-17 production did not reach significance (fig. S2G) and cell viability was unaffected as well (fig. S2H). The effects of the NLRP3 inhibitor could be fully reversed by the addition of rhIL-1β to cultures (Fig. 2G). Similarly, reduction of active caspase-1 activity by the specific inhibitor Z-YCAD-FMK repressed IL-1β and IFN-γ secretion (fig. S2I and Fig. 2H) and rhIL-1β provision normalized Th1 induction in these cultures. The role for IL-1β as critical autocrine 'Th1 supporter' is

reinforced by our observation that no IL-18 (which also depends on NLRP3 activation and can support Th1 responses (*37*) was measurable in our cultures and that addition of IL-18 binding protein had no effect on cytokine production (fig. S2J).

To further explore this pathway, we measured the effects of NLRP3 hyperactivity in $CD4^+$ T cells isolated from the blood of patients with distinct gain-of-function mutations in NLRP3 (patient characteristics are summarized in Table S3). This class of NLRP3 mutations is associated with a group of heritable monogenic syndromes known as cryopyrin-associated periodic syndromes (CAPS), characterized by excessive production of IL-1β from antigen presenting cells with recurrent fevers, skin rashes, joint and ocular inflammation and amyloidosis (*38*). Therapeutic suppression of the inflammatory responses can be achieved by IL-1R blockade with the IL-1 receptor antagonist anakinra, or canakinumab, a monoclonal antibody targeting IL-1R1 (*38*-*39*). Despite their medication regimen and the fact that cytokine production by immune cells from CAPS patients can vary with their respective 'flare status' (*40*), T cells from CAPS patients had significantly increased IL-1β secretion compared to sex- and age-matched healthy donors (fig. S2K), indicating that increased NLRP3 activity in $CD4^+$ T cells indeed induces heightened IL-1β secretion. We next performed a more in-depth analysis of T cell *in vitro* responses from another cohort of seven CAPS patients (Table S4). All patients had a naïve versus memory T cell distribution comparable to those of healthy donors (fig. S2L) and T cells from five patients showed also significantly increased IL-1β secretion upon activation (Fig. 2I). Furthermore, $CD4^+$ T cells from these patients produced substantially more IFN-γ when compared to T cells from sex- and age-matched healthy donors and a statistically significant correlation between increased IL-1β and IFN-γ secretion (Fig. 2J and K), but displayed significantly reduced IL-17 responses (Fig. 2L). Although caspase-1 activity was not significantly increased in the patients' T cells at the time point assessed (36 hours), the patients with highest IL-1β secretion also had the highest active caspase-1 levels (fig. S2M), and NLRP3 inhibition with MCC950 led to reduction of both IL-1β and IFN-γ secretion (Fig. 2M). Together, these data demonstrate that human $CD4^+$ T cells produce IL-1β in an NLRP3-dependent manner, that autocrine IL-1β generation supports IFN-γ secretion and, importantly, that dysregulation of this pathway occurs in human auto-inflammatory disease.

We next asked whether C5aR signalling could directly regulate NLRP3 activity in human $CD4^+$ T cells. C5aR2 blockade in CD3+CD46-activated T cells further increased *IL1B* but not *NLRP3* mRNA (fig. S3A and B). Enhanced IFN-γ in this context could be reversed by inhibition of NLRP3 with MCC950 (Fig. 3A) without affecting IL-4 or IL-17 production (fig. S3C). Pharmacological targeting of C5aR2 via either the dRA or a C5aR2 agonist revealed that C5aR2 negatively regulates active caspase-1 and mature IL-1β expression in T cells (Fig. 3B to D) but does not affect NLRP3 protein levels *per se* (fig. S3D). Silencing of *C5AR1* expression had also no effect on NLRP3 protein levels (fig. S3E) but reduced active caspase-1 (Fig. 3E) and IL-1β expression (Fig. 3F) and, importantly, the reduction of IFN-γ secretion after *C5AR1* gene silencing was 'rescued' by addition of rhIL-1β (Fig. 3G). Together these data suggest that CD46-mediated signals increase *NLRP3* mRNA expression in T cells while C5aR1 supports subsequent NLRP3 assembly and C5aR2 is a negative regulator of this process.

Reactive oxygen species (ROS) are 'classical' upstream stimulators of NLRP3 activation (*41*) and are strongly induced by C5aR1 in monocytes and neutrophils (*42*). Furthermore, generation of ROS within $CD4^+$ T cells is required for T cell activation and induction of IL-2, a key cytokine for Th1 biology (*43*). We therefore assessed whether autocrine C5 activity in T

cells regulates NLRP3 via ROS generation. We observed potent generation of ROS in anti-CD3 and anti-CD46-induced Th1 cells (Fig 3H) and poor Th1 induction in the presence of a ROS inhibitor (Fig. 3I). Inhibition of C5aR2 significantly increased ROS in T cells in contrast to silencing of C5aR1, which reduced ROS species (Fig. 3J). Enhanced IFN-γ production with C5aR2 blockade could be entirely reversed by the presence of an ROS inhibitor (Fig. 3I and fig. S3F), suggesting that NLRP3 activation in human T cells involves intracellular C5-driven ROS production.

To address the *in vivo* significance of NLRP3-driven autocrine IL-1β production by $CD4^+$ T cells, we analysed $CD4^+$ T cell responses of *Nlrp3*$^{-/-}$, *Il1a*$^{-/-}$/*Il1b*$^{-/-}$ and *Il1r1*$^{-/-}$ mice. Similar to human $CD4^+$ lymphocytes, $CD4^+$ cells from wild type (WT) mice expressed NLRP3 and IL-1β while neither NLRP3 nor IL-1β mRNA (Fig. 4A) and protein (fig. S4A) were detectable in T cells from respective gene deficient animals. We observed no difference in the proportion of naïve versus memory T cells or in T cell survival between WT and knockout strains (fig. S4B and C). However, upon *in vitro* CD3+CD28 activation, $CD4^+$ T cells from *Nlrp3*$^{-/-}$, *Il1a*$^{-/-}$/*Il1b*$^{-/-}$, and *Il1r1*$^{-/-}$ mice had a reduction of ~75 % in IFN-γ production when compared to T cells from WT animals (Fig. 4B); in contrast, IL-10, IL-4 and IL-17 production were unaffected in all three mouse mutant lines (fig. S4D). While activation of WT mouse T cells in the presence of the NLRP3 inhibitor MCC950 had no effect on cell viability (fig. S4E), only IFN-γ production was reduced significantly (Fig. 4C and fig. S4F), indicating that diminished IFN-γ secretion in the knockout T cells was not due to a developmental defect and that NLRP3 activity is required for normal IFN-γ induction. Moreover, both naïve and memory mouse $CD4^+$ T cells displayed a requirement for NLRP3-driven IL-1β activity for optimal IFN-γ secretion (fig. S4G and H). Using a lymphocytic choriomeningitis virus (LCMV) model (Fig. 4D) we demonstrated an *in vivo* role for NLRP3-driven IL-1β generation in Th1 responses during infection. Irradiated mice were reconstituted with equal parts bone marrow cells from WT mice together with either *Nlrp3*$^{-/-}$, *Il1a*$^{-/-}$/*Il1b*$^{-/-}$ or *Il1r1*$^{-/-}$ bone marrow cells, prior to infection with LCMV. Analysis of splenic $CD4^+$ T cells 12 days post infection revealed that all animals generated comparable numbers of GP66-77$^+$Ki67$^+$LCMV tetramer$^+$ cells at 12 days post infection (Fig. 4E and F), indicating that *Nlrp3*$^{-/-}$, *Il1a*$^{-/-}$/*Il1b*$^{-/-}$, and *Il1r1*$^{-/-}$ $CD4^+$ T cells survived normally. However, T cells deficient in any of these components displayed substantially reduced IFN-γ$^+$ virus-specific cells *in vivo* (with an average decrease of ~50%) (Fig. 4G and H). We further demonstrated the *in vivo* importance of autocrine NLPR3 activity in $CD4^+$ T cells, by assessing its influence on disease outcome in a $CD4^+$ T cell transfer model of colitis, where IL-1β and both Th1 and Th17 responses in the intestine have been shown to be involved (*44, 45*). Animals that had received *Nlrp3*$^{-/-}$ $CD4^+$ T cells developed more severe disease with significantly increased weight loss, reduction in colon length and higher disease scores when compared to mice injected with WT $CD4^+$ T cells (Fig. 4I to K). Similar to our observation in the LCMV model, colonic *Nlrp3*$^{-/-}$ T cells displayed a substantial reduction in IFN-γ production (average decrease ~45%) but also a concurrent increase in Th17 responses (Fig. 4L and M). These observations were confirmed using a $CD4^+$ T cell-driven model of graft versus host disease (GvHD) where mice receiving *Nlrp3*$^{-/-}$ T cells displayed more severe illness with reduced Th1 and increased Th17 induction (fig. S5A to D). Together these data demonstrate that the NLRP3 inflammasome mediates functionally important $CD4^+$ T cell intrinsic effects that control normal IFN-γ production and the Th1/Th17 balance during (at minimum) intestinal inflammation. These latter findings align with the observation that T cells from CAPS patients have indeed increased Th1 but decreased Th17 responses (fig. 2J and L).

Although $CD4^+$ T cells from *C5ar2*$^{-/-}$ mice have increased *in vitro* IFN-γ production which was reduced to normal levels by MCC950 treatment (fig. S5E) and *C5ar1*$^{-/-}$ mice have impaired *in vitro* and *in vivo* Th1 responses (*46*), there are clear species-specific differences in the relative contributions of complement receptor activities in IL-1β and/or IFN-γ induction. For example, the role and expression of anaphylatoxin receptors on mouse T cells remains a matter of controversy and mice lack expression of CD46 (or a full functional homologue) on somatic tissue (*47*). Further, as IL-1β also boosts the production of other cytokines including IL-4 and IL-17 (*35*), the engagement of the complement/NLRP3 inflammasome axis in T cells and its functional outcome could be context-dependent (infection, autoimmunity etc.). For example, Bruchard *et al*. recently observed a non-canonical function for NLRP3 in mouse $CD4^+$ T cells (they did not study human $CD4^+$ T cells), independent of inflammasome formation and IL-1β secretion, during Th2 induction and tumor growth (*48*).

In summary, we establish here that that NLRP3 inflammasome function is not confined to innate immune cells but is operative in adaptive $CD4^+$ T cells and, via autocrine IL-1β activity, required for the optimal production of the key host defense factor, IFN-γ. Further, and unexpectedly, NLRP3 assembly in human T cells requires TCR-induced intracellular C5 activation and stimulation of intracellular C5aR1. Secretion of intracellularly generated C5a/C5ades-Arg engages the surface-expressed 'alternative' C5aR2 which negatively controls NLRP3 activation (either through inhibition of C5aR1 or a yet undefined mechanism). We envisage that, whereas APC-derived NLRP3-activated IL-1β supports initial Th1 priming, maintenance of the Th1 phenotype during differentiation and migration into the periphery may rely on autocrine NLRP3 activity. IL-1β production by T cells, relative to myeloid cells, is comparatively low and tightly regulated by an autocrine C5aR1 vs. C5aR2 activation balance (fig. S6A), likely because rapid control of local IL-1β is critical to normal termination of Th1 responses: human Th1 cells co-induce IL-10 secretion in an CD46-dependent fashion during their contraction phase and failure of this 'IL-10 switch' underlies hyperactive Th1 responses observed in rheumatoid arthritis and multiple sclerosis (*3*, *9*). IL-1β is a strong suppressor of IL-10 production (*23*) and, accordingly, blockade of C5aR2 increased the IFN-γ:IL-10 ratio (fig. S6B). Further, IL-1β addition to cultures increased IFN-γ but blocked IL-10 secretion (fig. S6C) and T cells from CAPS patients have significantly reduced IFN-γ to IL-10 switching (fig. S6D).

Thus, the regulated crosstalk between intracellularly activated complement components ('complosome') and the NLRP3 inflammasome emerges as fundamental to human Th1 induction and regulation (and possibly regulating Th1/Th17 balance in inflammation). That established innate immune pathways previously not thought to be operative in adaptive immune cells are not only present but also are key in directing immunological responses is of substantial significance to our understanding of immunobiology and immune system evolution. Further, the possibility that this normal functional crosstalk may also be target of viral immune evasion strategies (*49*), suggests that the complement-NLRP3 axis in T cells could represent a novel therapeutic target for the modulation of IFN-γ responses in autoimmunity and infection. In this regard, it will be valuable to explore whether optimal production of IFN-γ by $CD8^+$ T cells (*50*), natural killer T (NKT) cells, and /or innate lymphoid type 1 (ILC1) cells also relies on autocrine complement-NLRP3 inflammasome activity.

References and Notes:

1. D. Ricklin, G. Hajishengallis, K. Yang, J. D. Lambris. Complement: a key system for immune surveillance and homeostasis. *Nat. Immunol.* 11(9):785-97 (2010).
2. K. M. Murphy, B. Stockinger. Effector T cell plasticity: flexibility in the face of changing circumstances. *Nat .Immunol.* 11(8):674-80 (2010).
3. J. Cardone, G. Le Friec, P. Vantourout, A. Robert, A. Fuchs, I. Jackson, T. Suddason, G. Lord, J. P. Atkinson, A. Cope, A. Hayday, C. Kemper. Complement regulator CD46 temporally regulates cytokine production by conventional and unconventional T cells. *Nat. Immunol.* 11, 862-71 (2010).
4. M. K. Liszewski, M. Kolev, G. Le Friec, M. Leung, P. G. Bertram, A. F. Fara, M. Subia, M. C. Pickerin, C. Drouet, S. Meri, T. P. Arstila, P. T. Pekkarine, M. Ma, A. Cope, T. Reinheckel, S. Rodriguez de Cordoba, B. Afzali, J. P. Atkinson, C. Kemper. Intracellular complement activation sustains T cell homeostasis and mediates effector differentiation. *Immunity* 12;39(6):1143-57 (2013).
5. G. Le Friec, D. Sheppard, P. Whiteman, C. M. Karsten, S. A. Shamoun, A. Laing, L. Bugeon, M. J. Dallman, T. Melchionna, C. Chillakuri, R. A. Smith, C. Drouet, L. Couzi, V. Fremeaux-Bacchi, J. Köhl, S. N. Waddington, J. M. McDonnell, A. Baker, P. A. Handford, S. M. Lea, C. Kemper. The CD46-Jagged1 interaction is critical for human TH1 immunity. *Nat. Immunol.* 13(12):1213-21 (2012).
6. H. Yamamoto, A. F. Fara, P. Dasgupta, C. Kemper. CD46. The multitasker of complement proteins. *Intern. J. Biochem. Cell Biol*. 45(12):2808-20 (2013).
7. M. Kolev, S. Dimeloe, G. Le Friec, A. Navarini, G. Arbore, G. A. Povoleri, M. Fischer, R. Belle, J. Loeliger, L. Develioglu, G. R. Bantug, J. Watson, L. Couzi, B. Afzali, P. Lavender, C. Hess, C. Kemper. Complement Regulates Nutrient Influx and Metabolic Reprogramming during Th1 Cell Responses. *Immunity* 42(6):1033-47 (2015).
8. A. Ghannam, M. Pernollet, J. L. Fauquert, N. Monnier, D. Ponard, M. B. Villiers, J. Péguet-Navarro, A. Tridon, J. Lunardi, D. Gerlier, C. Drouet. Human C3 deficiency associated with impairments in dendritic cell differentiation, memory B cells, and regulatory T cells. *J. Immunol.* 181(7):5158-66 (2008).
9. A. L. Astier, G. Meiffren, S. Freeman, D. A. Hafler. Alterations in CD46-mediated Tr1 regulatory T cells in patients with multiple sclerosis. *J. Clin .Invest.* 116(12):3252-7 (2006).
10. J. V. Sarma, P. A. Ward. New developments in C5a receptor signaling. *Cell Health Cytoskelet.* 4, 73-82 (2012).
11. A. M. Scola, K. O. Johswich, B. P. Morgan, A. Klos, P. N. Monk. The human complement fragment receptor, C5L2, is a recycling decoy receptor. *Mol. Immunol.* 46, 1149-62 (2009).
12. N. P. Gerard, B. Lu, P. Liu, S. Craig, Y. Fujiwara, S. Okinaga, C. Gerard. An anti-inflammatory function for the complement anaphylatoxin C5a-binding protein, C5L2. *J. Biol. Chem.* 280, 39677-80 (2005).
13. C. E. Bamberg, C. R. Mackay, H. Lee, D. Zahra, J. Jackson, Y. S. Lim, P. L. Whitfeld, S. Craig, E. Corsini, B. Lu, C. Gerard, N. P. Gerard. The C5a receptor (C5aR) C5L2 is a modulator of C5aR-mediated signal transduction. *J. Biol. Chem.* 285, 7633-44 (2010).

14. R. Li, L. G. Coulthard, M. C. W, S. M. Taylor, T. M. Woodruff. C5L2: a controversial receptor of complement anaphylatoxin, C5a. *FASEB J.* 27, 855-64 (2013).

15. D.E. Croker, R. Halai, D.P. Fairlie, M.A. Cooper. C5a, but not C5a-des Arg induces upregulation of heteromer formation between its complement C5a receptors C5aR and C5L2. *Immunol. & Cell Biol.* 91(10): 625-33 (2013).

16. C. Vogel, E.M. Marcotte. Insights into the regulation of protein abundance from proteomic and transcriptomic analyses. *Nat Rev Genet*. 13(4):227-32 (2012).

17. T. M. Woodruff, J. W. Cran, L. M. Proctor, K. M. Bulle, A. B. She, K. de Vos, S. Pollitt, H. M. Williams, I. A. Shiels, P. N. Monk, S. M. Taylor. Therapeutic activity of C5a receptor antagonists in a rat model of neurodegeneration. *FASEB J.* 20(9):1407-17 (2006).

18. M. Otto, H. Hawlisch, P. N. Monk, M. Müller, A. Klos, C. L. Karp, J. Köhl. C5a mutants are potent antagonists of the C5a receptor (CD88) and of C5L2: position 69 is the locus that determines agonism or antagonism. *J. Biol. Chem.* 279(1):142-51 (2004).

19. P. N. Monk, M. L. Bellows-Peterson, J. Smadbeck, C. A. Floudas, C. A. Kieslich, D. Morikis, T. M. Woodruff. De novo protein design of agonists and antagonists of C5a receptors. *Immunobiology* 217 (11) 1162–1163 (2012).

20. A. Kastbom, D. Verma, P. Eriksson, T. Skogh, G. Wingren, P. Söderkvist. Genetic variation in proteins of the cryopyrin inflammasome influences susceptibility and severity of rheumatoid arthritis (the Swedish TIRA project). *Rheumatology* 47:415–417 (2008).

21. A. Pontillo, L. Brandao, R. Guimaraes, L. Segat, J. Araujo, S. A. Crovella. Two SNPs in NLRP3 gene are involved in the predisposition to type-1 diabetes and celiac disease in a pediatric population from northeast Brazil. *Autoimmunity* 43(8):583-9 (2010).

22. P. J. Shaw, M. F. McDermott and T. D. Kanneganti. Inflammasomes and autoimmunity. *Trends Mol. Med.* 17(2): 57–64 (2011).

23. C. E. Zielinski, F. Mele, D. Aschenbrenner, D. Jarrossay, F. Ronchi, M. Gattorno, S. Monticelli, A. Lanzavecchia, F. Sallusto. Pathogen-induced human TH17 cells produce IFN-γ or IL-10 and are regulated by IL-1β. *Nature* 484(7395):514-8 (2012).

24. C. E. Sutton, C. Brereton, B. Keogh, K. H. Mills, E. C. Lavelle. A crucial role for interleukin (IL)-1 in the induction of IL-17-producing T cells that mediate autoimmune encephalomyelitis. *J. Exp. Med.* 203, 1685–1691 (2006).

25. D. A. Rao, K. J. Tracey, J. S. Pober. IL-1alpha and IL-1beta are endogenous mediators linking cell injury to the adaptive alloimmune response. *J. Immunol.* 179(10):6536-46 (2007).

26. C. E. Sutton, S. J. Lalor, C. M. Sweeney, C. F. Brereton, E. C. Lavelle, K. H. Mills. Interleukin-1 and IL-23 induce innate IL-17 production from γδ T cells, amplifying Th17 responses and autoimmunity. *Immunity* 31, 331–341 (2009).

27. D. Schenten, S. A. Nish, S. Yu, X. Yan, H. K. Lee, I. Brodsky, L. Pasman, B. Yordy, F. T. Wunderlich, J. C. Brüning, H. Zhao, R. Medzhitov. Signaling through the adaptor molecule MyD88 in CD4+ T cells is required to overcome suppression by regulatory T-cells. *Immunity* 40(1):78-90 (2014).

28. W. P. Arend, G. Palmer, C, Gabay. IL-1, IL-18, and IL-33 families of cytokines. *Immunol. Rev.* 223:20-38 (2008).

29. F. Martinon, J. Tschopp. NLRs join TLRs as innate sensors of pathogens. *Trends Immunol.* 26(8):447-54 (2005).

30. J. K. Dowling JK, L. A. O'Neill. Biochemical regulation of the inflammasome. Crit. Rev. *Biochem. Mol. Biol.* 47, 424-43 (2012).

31. C. A. Dinarello. Biologic basis for interleukin-1 in disease. *Blood* 15;87(6):2095-147 (1996).

32. M. T. Heneka, M. P. Kummer, A. Stutz, A. Delekate, S. Schwartz, A. Vieira-Saecker, A. Griep, D. Axt, A. Remus, T. C. Tzeng, E. Gelpi, A. Halle, M. Korte, E. Latz, D. T. Golenbock. NLRP3 is activated in Alzheimer's disease and contributes to pathology in APP/PS1 mice. *Nature*. 493(7434):674-8 (2013).

33. K. Shahzad, F. Bock, W. Dong, H. Wang, S. Kopf, S. Kohli, M. M. Al-Dabet, S. Ranjan, J. Wolter, C. Wacker, R. Biemann, S. Stoyanov, K. Reymann, P. Söderkvist, O. Groß, V. Schwenger, S. Pahernik, P. P. Nawroth, H. J. Gröne, T. Madhusudhan, B. Isermann. **Nlrp3-inflammasome** activation in non-myeloid-derived cells aggravates diabetic nephropathy. *Kidney Int*. 87(1):74-84 (2015).

34. W. A. Tseng, T. Thein, K. Kinnunen, K. Lashkari, M. S. Gregory, P. A. D'Amore, B. R. Ksander. NLRP3 inflammasome activation in retinal pigment epithelial cells by lysosomal destabilization: implications for age-related macular degeneration. *Invest Ophthalmol Vis. Sci.* 54(1):110-20 (2013).

35. S. Z. Ben-Sasson, J. Hu-Li, J. Quiel, S. Cauchetaux, M. Ratner, I. Shapira, C. A. Dinarello, W. E. Paul. IL-1 acts directly on CD4 T cells to enhance their antigen-driven expansion and differentiation. *Proc. Natl. Acad. Sci. U S A.* 28;106(17):7119-24 (2009).

36. R. C. Coll, A. A. Robertson, J. J. Chae, S. C. Higgin, R. Muñoz-Planill, M. C. Inserra, I. Vetter, L. S. Dungan,B. G. Monks, A. Stutz, D. E. Croker, M. S. Butle, M. Haneklaus, C. E. Sutton, G. Núñez, E. Latz, D. L. Kastner, K. H. Mills, S. L. Masters, K. Schroder, M. A. Cooper, L. A. O'Neill LA. A small-molecule inhibitor of the NLRP3 inflammasome for the treatment of inflammatory diseases. *Nat. Med.* 21(3):248-55 (2015).

37. H. Okamura, H. Tsutsi, T. Komatsu, M. Yutsudo, A. Hakura, T. Tanimoto, K. Torigoe, T. Okura, Y. Nukada, K. Hattori, K. Akita, M. Namba, F. Tanabe, K. Konishi, S. Fukuda and M. Kurimoto. Cloning of a new cytokine that induces IFN-gamma production by T cells. *Nature*. 378(6552):88-91 (1995).

38. P. Menu, J. E. Vince. The NLRP3 inflammasome in health and disease: the good, the bad and the ugly. *Clin. Exp. Immunol.* 166(1):1-15.34 (2011).

39. H. J. Lachmann, P. Lowe, S. D. Felix, C. Rordorf, K. Leslie, S. Madhoo, H. Wittkowski, S. Bek, N. Hartmann, S. Bosset, P. N. Hawkins, T. Jung. In vivo regulation of interleukin 1beta in patients with cryopyrin-associated periodic syndromes. *J. Exp. Med.* 206(5):1029-36 (2009).

40. S. Carta, F. Penco, R. Lavieri, A. Martini, C.A. Dinarello, M Gattorno, A. Rubartelli. Cell stress increases ATP release in NLRP3 inflammasome-mediated autoinflammatory diseases, resulting in cytokine imbalance. *Proc Natl Acad Sci U S A*. 112(9):2835-40 (2015).

41. K. Schroder, R. Zhou, J. Tschopp. The NLRP3 inflammasome: a sensor for metabolic danger? *Science* 327(5963):296-300 (2010).

42. O. Samstad, N. Niyonzima, S. Nymo, M. H. Aune, L. Ryan, S. S. Bakke, K. T. Lappegård, O. L. Brekke, J. D. Lambris, J. K. Damås, E. Latz, T. E. Mollnes, T. Espevik. Cholesterol crystals induce complement-dependent inflammasome activation and cytokine release. *J. Immunol.* 192(6):2837-45.70 (2014).

43. L. A. Sena, S. Li, A. Jairaman, M. Prakriya, T. Ezponda, D. A. Hildeman, C. R. Wang, P. T. Schumacker, J. D. Licht, H. Perlman, P. J. Bryce, N. S. Chandel. Mitochondria are required for antigen-specific T cell activation through reactive oxygen species signaling. *Immunity* 38(2):225-36 (2013).

44. M. Coccia, O. J. Harrison, C. Schiering, M. J. Asquith, B. Becher, F. Powrie, K. J. Maloy. IL-1β mediates chronic intestinal inflammation by promoting the accumulation of IL-17A secreting innate lymphoid cells and CD4(+) Th17 cells. *J Exp. Med*. 209(9):1595-609 (2012).

45. M. F. Neurath. Cytokines in inflammatory bowel disease. *Nat. Rev. Immunol.* 14(5):329-42 (2014).

46. M. G. Strainic, J. Liu, D. Huang, F. An, P. N. Lalli, N. Muqim, V. S. Shapiro, G. R. Dubyak, P. S. Heeger, M. E. Medof. Locally produced complement fragments C5a and C3a provide both costimulatory and survival signals to naive CD4+ T cells. *Immunity* 28, 425-35 (2008).

47. Kolev M, Le Friec G, Kemper C. Complement: tapping into new sites and effector systems. *Nat Rev Immunol.* 14(12):811-20 (2014).

48. M. Bruchard, C. Rebé, V. Derangère, D. Togbé, B. Ryffel, R. Boidot, E. Humblin, A. Hamman, F. Chalmin, H. Berger, A. Chevriaux, E. Limagne, L. Apetoh, F. Végran, F. Ghiringhelli. The receptor NLRP3 is a transcriptional regulator of T_H2 differentiation. *Nat. Immunol.* 16(8):859-70 (2015).

49. G. Doitsh, N. L. Galloway, X. Geng, Z. Yang, K. M. Monroe, O. Zepeda, P. W. Hunt, H. Hatano, S. Sowinski,I. Muñoz-Arias, W. C. Greene. Cell death by pyroptosis drives CD4 T-cell depletion in HIV-1 infection. *Nature* 505(7484):509-14 (2014).

50. S.Z. Ben-Sasson, A. Hogg, J. Hu-Li, P. Wingfield, X. Chen, M. Crank, S. Caucheteux, M. Ratner-Hurevich, J.A. Berzofsky, R. Nir-Paz, W.E. Paul. IL-1 enhances expansion, effector function, tissue localization, and memory response of antigen-specific CD8 T cells. *J. Exp Med.* 210(3):491-502 (2013).

51. Mayer-Barber KD, Andrade BB, Oland SD, Amaral EP, Barber DL, Gonzales J, Derrick SC, Shi R, Kumar NP, Wei W, Yuan X, Zhang G, Cai Y, Babu S, Catalfamo M, Salazar AM, Via LE, Barry CE 3rd, Sher A. Host-directed therapy of tuberculosis based on interleukin-1 and type I interferon crosstalk. *Nature* 511(7507):99-103 (2014).

52. Wang, G., Liszewski, M.K., Chan, A.C., and Atkinson, J.P. Membrane cofactor protein (MCP; CD46): isoform-specific tyrosine phosphorylation. *J. Immunol* 164, 1839-1846 (2000).

53. Rasheed MA, Latner DR, Aubert RD, Gourley T, Spolski R, Davis CW, Langley WA, Ha SJ, Ye L, Sarkar S, Kalia V, Konieczny BT, Leonard WJ, Ahmed R. Interleukin-21 is a critical

cytokine for the generation of virus-specific long-lived plasma cells. *J. Virol*. 87(13):7737-46 (2013).

54. V. Valatas, J. He, A. Rivollier, G. Kolios, K. Kitamura, B. L. Kelsall. Host-dependent control of early regulatory and effector T-cell differentiation underlies the genetic susceptibility of RAG2-deficient mouse strains to transfer colitis. *Mucosal Immunol*. 6(3):601-11 (2013).
55. D. Bock D, U. Martin, S. Gärtner, C. Rheinheimer, U. Raffetseder, L. Arseniev, M. D. Barker, P. N. Monk, W. Bautsch, J. Köhl, A. Klos. The C terminus of the human C5a receptor (CD88) is required for normal ligand-dependent receptor internalization. *Eur. J. Immunol.* 27(6):1522-9 (1997).
56. Subramanian A, Tamayo P, Mootha VK, Mukherjee S, Ebert BL, Gillette MA, Paulovich A, Pomeroy SL, Golub TR, Lander ES, Mesirov JP. Gene set enrichment analysis: A knowledge-based approach for interpreting genome-wide expression profiles. *Proc. Natl. Acad. Sci. U.S.A*. 102 (43): 15545–50 (2005).

Acknowledgments: We thank the healthy volunteers and the patients for their support, A. Fara and J. Sumner (King's College London, United Kingdom) for initial contribution to the C5aR2 antagonism studies and Prof. Y. Iwakura (Tokyo University, Japan) for providing the combined *Il1a/Il1b*$^{-/-}$ mice. The MHC class II tetramer to LCMV (GP66-77) was kindly provided by the NIH tetramer core. We thank the Nikon Imaging Centre and the Genomics Centre at King's College London (London, UK).

This work was supported by the MRC Centre grant MR/J006742/1, an EU-funded Innovative Medicines Initiative BTCURE (C.K. and A.C.), a Wellcome Trust Investigator Award (C.K), a Wellcome Trust Intermediate Clinical Fellowship award (B.A.), the King's Bioscience Institute at King's College London (G.A.), the National Institute for Health Research (NIHR) Biomedical Research Centre based at Guy's and St Thomas' NHS Foundation Trust and King's College London, and by the Division of Intramural Research, National Heart, Lung, and Blood Institute, NIH and the intramural research program of NIAID, NIH.

Competing financial interest

The authors declare no competing financial interests.

Figure Legends

Fig. 1. Autocrine activation of C5a receptors regulates IFN-γ production by human CD4$^+$ T cells. (**A** and **B**) Intracellular C5 and C5a generation in CD4$^+$ T lymphocytes, left non-activated or activated (36 hours) with α-CD3, α-CD3 + α-CD28 or α-CD3 + α-CD46 by flow cytometry (**A**) and confocal microscopy (**B**) (data representative of n=3). (**C**) RT-PCR analysis for *C5AR1* and *C5AR2* mRNA in resting human CD4$^+$ cells and monocytes (n=4, donors D1-D4, endogenous control *ACTB*). (**D**) Intracellular immunofluorescence on resting T cells and monocytes with antibodies to C5aR1 (green) and C5aR2 (red) (data representative of n=3). (**E**) C5aR1 and C5aR2 protein amounts in T cells with expression normalized to respective isotype control staining for each donor (ΔMFI ± SEM, n=6). (**F**) Flow cytometry for C5aR1 and C5aR2 on resting T cells and monocytes, with representative histogram plots shown (n=6). (**G**) Binding of radioactively-labelled ^{125}I-C5a in absence or presence of non-labelled 'cold' C5a as competitor to resting or α-CD3 + α-CD46 activated (4 hours) T cells (n=6). (**H**) IFN-γ secretion in non-activated (NA) and activated (36 hours) CD4$^+$ T cells in the absence or presence of either a C5aR1/C5aR2 double receptor antagonist (n=9), a C5aR2 agonist (n=8) or a C5aR1 antagonist (n=7). (**I**) IFN-γ production by T cells transfected with C5aR1-specific siRNA or a scrambled control siRNA (Ctrl. siRNA) 36 hours post activation (n=7). Error bar graphs represent mean ± SEM. **p* <0.05, ***p* <0.01, *****p* <0.0005.

Fig. 2 NLRP3 inflammasome activation occurs in CD4$^+$ T cells and enhances IFN-γ production. (**A**) Gene Set Enrichment Analysis (GSEA) for inflammasome-related genes in CD4$^+$ T cells after α-CD3 + α-CD46 activation (2 hours) compared to resting cells (donors D1-D3). (**B**) Heatmap depicting leading edge analysis (the core enriched genes) of the data in (**A**). (**C**) NLRP3 immunoblot (upper panel) and immunofluorescence (lower panel) on CD4$^+$ lymphocytes and monocytes. (**D**) NLRP3, activated caspase-1 and total IL-1β protein expression in activated CD4$^+$ cells (data representative of n=3). **(E)** Representative immunofluorescence co-staining for NLRP3 (green) and ASC (red) on resting and α-CD3 + α-CD46 activated T cells (r = Pearson's correlation coefficient between NLRP3 and ASC fluorescence, n=3). **(F** and **G)** IFN-γ production by resting (NA) and activated CD4$^+$ T cells with or without MCC950 addition (n=7) (**F**) and with or without rhIL-1β supplementation (n=3) (**G**). (**H**) IFN-γ production in presence of the specific caspase-1 inhibitor Z-YVAD-FMK with or without rhIL-1β addition. (**I**) IL-1β secretion from resting and α-CD3 + α-CD46 activated CD4$^+$ cells from seven patients with CAPS (P8-P14, individual values) and five healthy sex- and age-matched donors (HD5-HD9, combined values). (**J**) IFN-γ secretion by resting and activated CD4$^+$ cells from seven patients with CAPS (P8-P14) and seven sex- and age-matched healthy donors (HD5-11). (**K**) Correlation between IL-1β and IFN-γ production in T cells from patients P8-P14 upon α-CD3 + α-CD46 activation (Spearman correlation analysis). (**L**) IL-17 production by resting and activated T cells from CAPS patients P8-P14 and healthy donors H5-H11. (**M**) IFN-γ and IL-1β secretion by CD4$^+$ T cells from P8, P11 and P14 post α-CD3+α-CD46 activation with or without MCC950 treatment (% normalized to non-treated). Analyses on (D - M) were performed at 36 hours post-activation. Error bar graphs represent mean ± SEM. **p* <0.05, ***p* <0.01, ****p* <0.001, *****p* <0.0005.

Fig. 3 C5a receptors regulate NLRP3 activation to modulate IFN-γ responses. (**A**) IFN-γ production in $CD4^+$ T cells either left non-activated (NA) or activated as depicted with or without addition of the C5aR1/C5aR2 antagonist and/or MCC950 (n=3). (**B** and **C**) Measurement of active caspase-1-positive $CD4^+$ T cells activated with α-CD3 + α-CD46 with or without MCC950, the C5aR1/C5aR2 antagonist or the C5aR2 agonist (n=3) (**B**) and statistical analyses of data obtained (**C**). (**D**) Corresponding IL-1β secretion in activated $CD4^+$ cells treated as in (B) (n=5). (**E** and **F**) Active caspase-1 levels (**E,** n=4) and IL-1β secretion (**F,** n=7) in T cells after transfection with either C5aR1-specific siRNA or scrambled control (Ctrl.) siRNA. (**G**) IFN-γ production in activated $CD4^+$ T cells after transfection with C5aR1-specific siRNA or a scrambled control siRNA (Ctrl. siRNA) with or without addition of rhIL-1β (n=3). (**H**) ROS production in $CD4^+$ T cells activated under the depicted conditions (data representative of n=3). (**I**) IFN-γ production from $CD4^+$ T cells left non-activated or activated as indicated with and without a specific ROS inhibitor and/or the C5aR1/C5aR2 antagonist (n=3). (**J**) ROS production in α-CD3 + α-CD46 activated $CD4^+$ cells with or without the C5aR1/C5aR2 double antagonist (left panel) or after transfection with *C5aR1*-specific siRNA (right panel) (data representative of n=3). Analyses were performed at 36 hours post-activation. Error bar graphs represent mean ± SEM. **p* <0.05, ***p* <0.01, ****p* <0.001.

Fig. 4 NLRP3 function in $CD4^+$ T cells is required for optimal IFN-γ responses *in vivo*. (**A**) RT-PCR analysis on $CD4^+$ T cells isolated from wild type (WT), *Nlrp3*$^{-}$, combined *Il1a*$^{-/-}$ and *Il1b*$^{-/-}$ (*Il1a/b*$^{-/-}$) and *Il1r1*$^{-/-}$ mice for corresponding gene mRNA expression. (**B**) Cytokine secretion from $CD4^+$ T cells isolated from WT and knock out mice at 96 hours post α-CD3 + α-CD28 activation (n=3). (**C**) Cytokine production from $CD4^+$ T cells from WT and *Nlrp3*$^{-/-}$mice post α-CD3 + α-CD28 activation (96 hours) with or without addition of MCC950 (n=4). (**D**) Schematic of the acute Lymphocytic Choriomeningitis Virus (LCMV) infection model employed in this study. (**E** and **F**) Percentage of LCMV tetramer-positive $CD4^+$ T cells isolated from the spleens of the three bone-marrow chimeric mice groups used 12 days post infection (**E**) and percentages of $Ki67^+GP66\text{-}77^+$/tetramer-positive cells (**F**). (**G** and **H**) Representative intracellular IFN-γ staining in splenic $CD4^+$ T cells of one mouse from each group after LCMV peptide re-stimulation (5 hours) (**G,** n=6) with corresponding statistical analyses (**H**, n=6). (**I-M**) Naïve splenic $CD25^-CD45RB^{hi}$ $CD4^+$ T cells from WT or *Nlpr3*$^{-/-}$ mice were transferred into C57BL/10 $RAG2^{-/-}$ mice. (**I**) Weight change over the course of colitis induction. (**J**) Colon length at the study endpoint. (**K**) Inflammation score of the colons according to blinded histological analysis with assessment of inflammation (left panel), epithelial damage (middle panel) and muscular immune cell infiltration (right panel). **(L-M)** Intracellular IFN-γ and IL-17A staining of colonic $CD4^+$ T cells at the study endpoint after overnight α-CD3 + α-CD28 stimulation and brefeldin A and monensin addition for 5 hours (Gated on live $CD4^+$ $Thy1.2^+$ T cells). Representative flow cytometric plots **(L)** with corresponding statistical analysis shown from 2 combined independent experiments (**M**, n=13 WT, 15 KO). Error bar graphs represent mean ± SEM **p* <0.05, ***p* <0.01.

Supplementary Materials:

Materials and Methods

Figures S1-S6

Tables S1-S5

Fig. 1

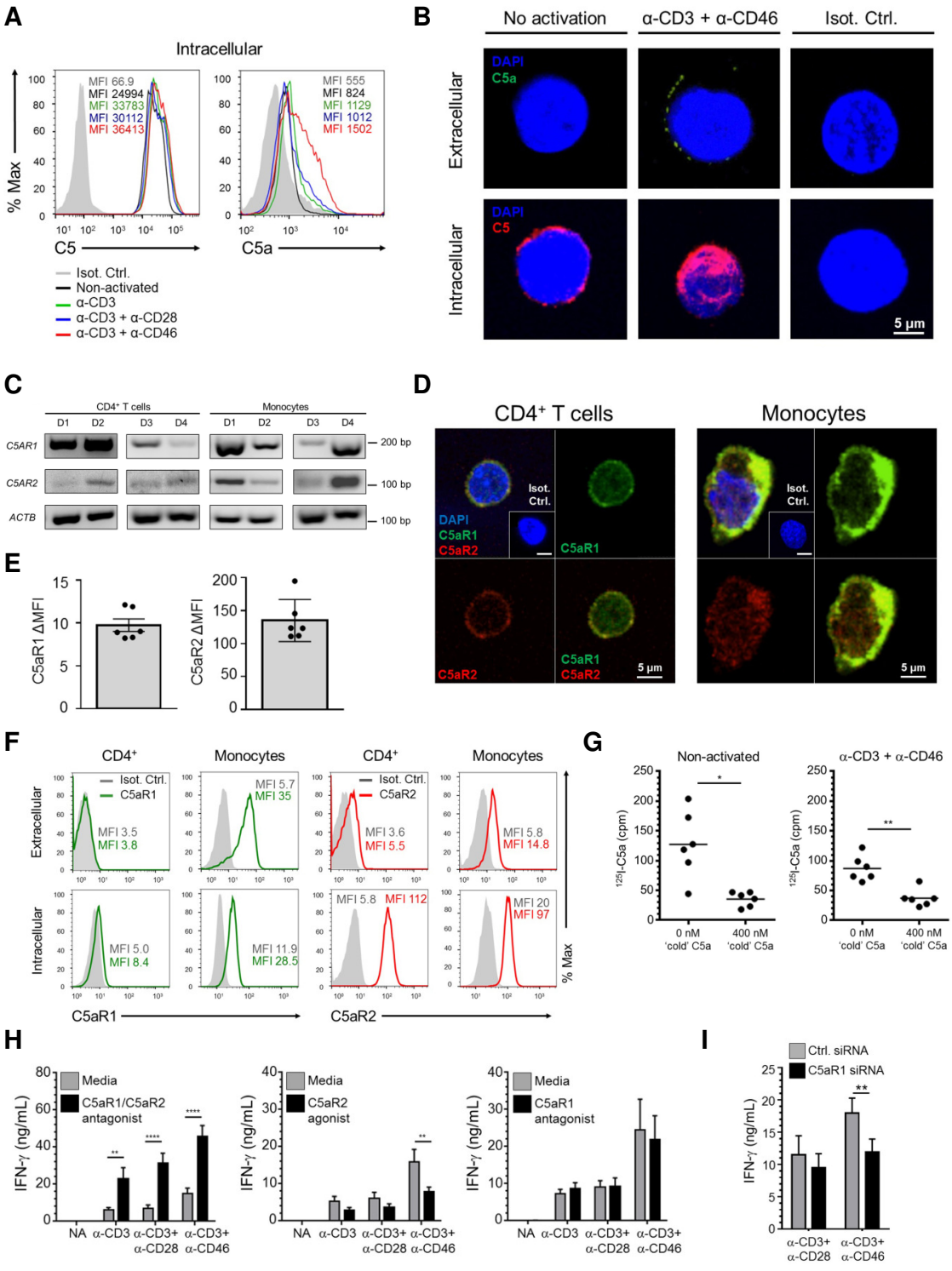
A
Intracellular
% Max
MFI 66.9
MFI 24994
MFI 33783
MFI 30112
MFI 36413
MFI 555
MFI 824
MFI 1129
MFI 1012
MFI 1502
C5
C5a
Isot. Ctrl.
Non-activated
α-CD3
α-CD3 + α-CD28
α-CD3 + α-CD46
B
No activation
α-CD3 + α-CD46
Isot. Ctrl.
Extracellular
Intracellular
DAPI
C5a
C5
5 µm
C
CD4⁺ T cells
Monocytes
D1
D2
D3
D4
C5AR1
C5AR2
ACTB
200 bp
100 bp
100 bp
D
CD4⁺ T cells
Monocytes
Isot. Ctrl.
DAPI
C5aR1
C5aR2
5 µm
E
C5aR1 ΔMFI
C5aR2 ΔMFI
F
CD4⁺
Monocytes
Extracellular
Intracellular
Isot. Ctrl.
C5aR1
C5aR2
MFI 3.5
MFI 3.8
MFI 5.7
MFI 35
MFI 3.6
MFI 5.5
MFI 5.8
MFI 14.8
MFI 5.0
MFI 8.4
MFI 11.9
MFI 28.5
MFI 5.8
MFI 112
MFI 20
MFI 97
% Max
C5aR1
C5aR2
G
Non-activated
α-CD3 + α-CD46
125I-C5a (cpm)
0 nM 'cold' C5a
400 nM 'cold' C5a
H
IFN-γ (ng/mL)
Media
C5aR1/C5aR2 antagonist
C5aR2 agonist
C5aR1 antagonist
NA
α-CD3
α-CD3+ α-CD28
α-CD3+ α-CD46
I
Ctrl. siRNA
C5aR1 siRNA
IFN-γ (ng/mL)
α-CD3+ α-CD28
α-CD3+ α-CD46

Fig. 2

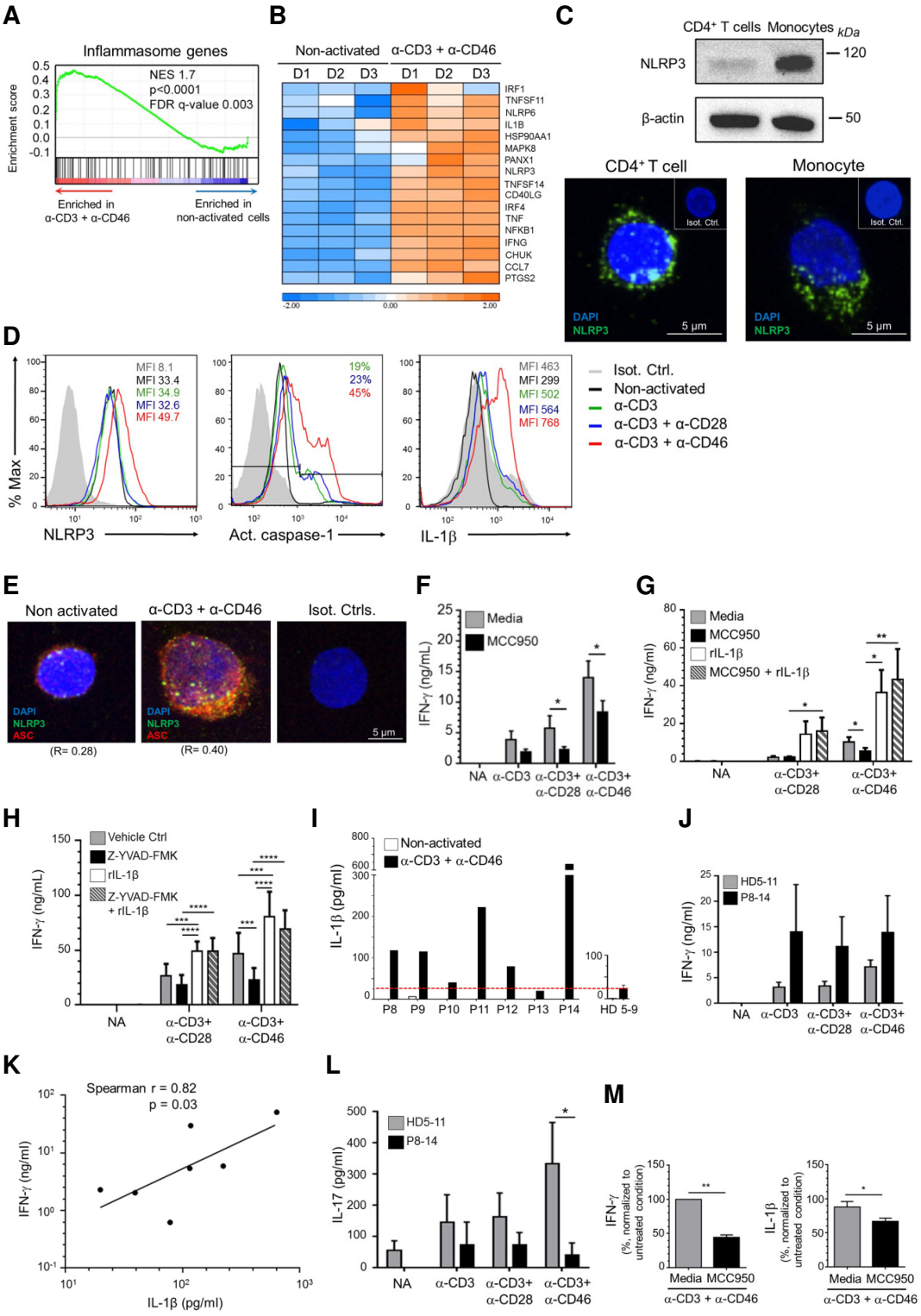
A
Inflammasome genes
NES 1.7
p<0.0001
FDR q-value 0.003
Enrichment score
Enriched in α-CD3 + α-CD46
Enriched in non-activated cells
B
Non-activated
α-CD3 + α-CD46
D1 D2 D3 D1 D2 D3
IRF1
TNFSF11
NLRP6
IL1B
HSP90AA1
MAPK8
PANX1
NLRP3
TNFSF14
CD40LG
IRF4
TNF
NFKB1
IFNG
CHUK
CCL7
PTGS2
C
CD4+ T cells Monocytes kDa
NLRP3
120
β-actin
50
CD4+ T cell
Monocyte
Isot. Ctrl.
DAPI
NLRP3
5 μm
D
% Max
MFI 8.1
MFI 33.4
MFI 34.9
MFI 32.6
MFI 49.7
NLRP3
19%
23%
45%
Act. caspase-1
MFI 463
MFI 299
MFI 502
MFI 564
MFI 768
IL-1β
Isot. Ctrl.
Non-activated
α-CD3
α-CD3 + α-CD28
α-CD3 + α-CD46
E
Non activated
α-CD3 + α-CD46
Isot. Ctrls.
DAPI
NLRP3
ASC
(R= 0.28)
(R= 0.40)
5 μm
F
Media
MCC950
IFN-γ (ng/mL)
NA
α-CD3
α-CD3+ α-CD28
α-CD3+ α-CD46
G
Media
MCC950
rIL-1β
MCC950 + rIL-1β
IFN-γ (ng/ml)
NA
α-CD3+ α-CD28
α-CD3+ α-CD46
H
Vehicle Ctrl
Z-YVAD-FMK
rIL-1β
Z-YVAD-FMK + rIL-1β
IFN-γ (ng/mL)
NA
α-CD3+ α-CD28
α-CD3+ α-CD46
I
Non-activated
α-CD3 + α-CD46
IL-1β (pg/ml)
P8 P9 P10 P11 P12 P13 P14
HD 5-9
J
HD5-11
P8-14
IFN-γ (ng/ml)
NA
α-CD3
α-CD3+ α-CD28
α-CD3+ α-CD46
K
Spearman r = 0.82
p = 0.03
IFN-γ (ng/ml)
IL-1β (pg/ml)
L
HD5-11
P8-14
IL-17 (pg/ml)
NA
α-CD3
α-CD3+ α-CD28
α-CD3+ α-CD46
M
IFN-γ (%, normalized to untreated condition)
Media MCC950
α-CD3 + α-CD46
IL-1β (%, normalized to untreated condition)
Media MCC950
α-CD3 + α-CD46

Fig. 3

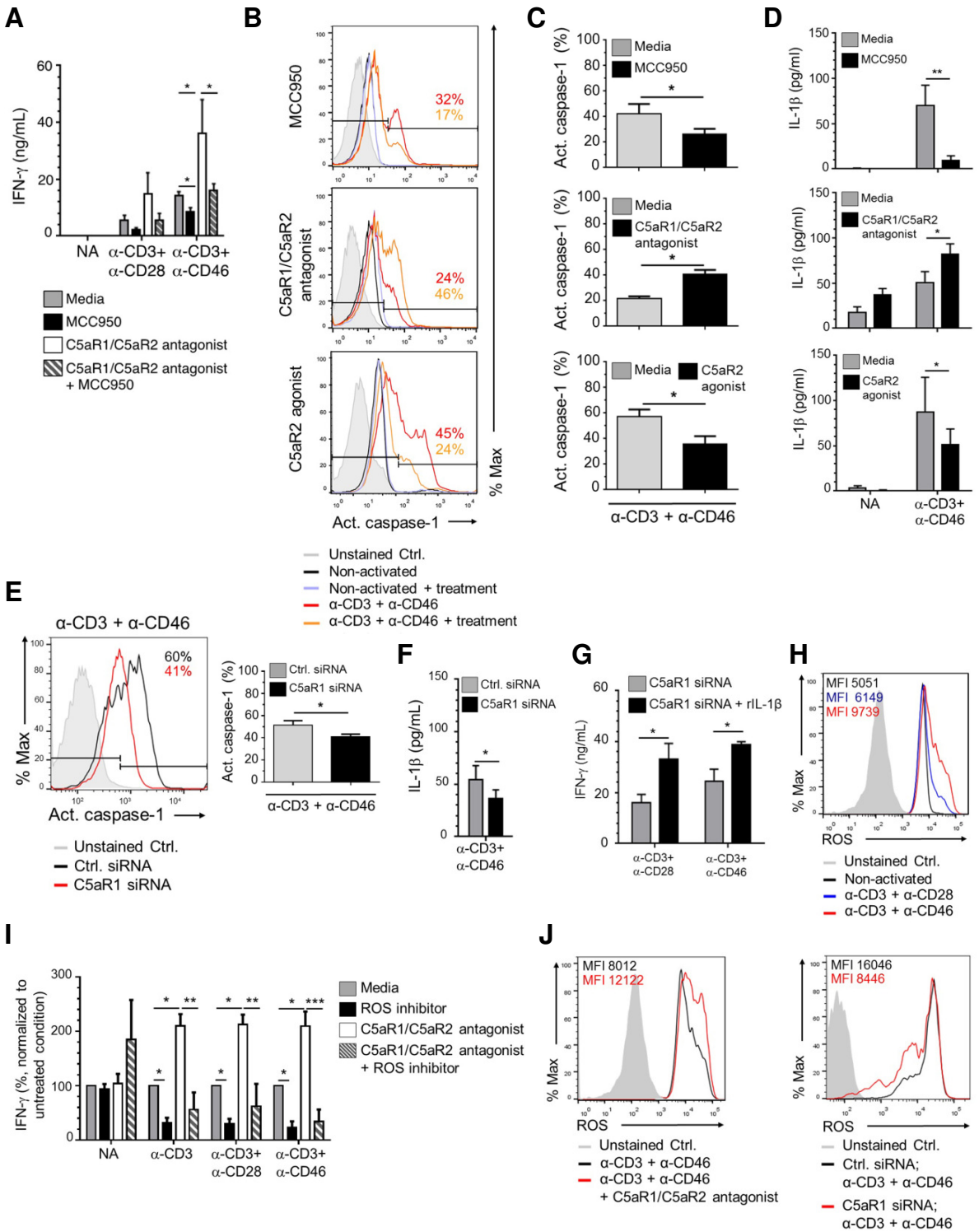
A
IFN-γ (ng/mL)
NA
α-CD3+ α-CD28
α-CD3+ α-CD46
Media
MCC950
C5aR1/C5aR2 antagonist
C5aR1/C5aR2 antagonist + MCC950
B
MCC950
32%
17%
C5aR1/C5aR2 antagonist
24%
46%
C5aR2 agonist
45%
24%
% Max
Act. caspase-1
Unstained Ctrl.
Non-activated
Non-activated + treatment
α-CD3 + α-CD46
α-CD3 + α-CD46 + treatment
C
Act. caspase-1 (%)
Media
MCC950
C5aR1/C5aR2 antagonist
C5aR2 agonist
α-CD3 + α-CD46
D
IL-1β (pg/ml)
Media
MCC950
C5aR1/C5aR2 antagonist
C5aR2 agonist
NA
α-CD3+ α-CD46
E
α-CD3 + α-CD46
60%
41%
% Max
Act. caspase-1
Unstained Ctrl.
Ctrl. siRNA
C5aR1 siRNA
Act. caspase-1 (%)
Ctrl. siRNA
C5aR1 siRNA
α-CD3 + α-CD46
F
IL-1β (pg/mL)
Ctrl. siRNA
C5aR1 siRNA
α-CD3+ α-CD46
G
IFN-γ (ng/mL)
C5aR1 siRNA
C5aR1 siRNA + rIL-1β
α-CD3+ α-CD28
α-CD3+ α-CD46
H
MFI 5051
MFI 6149
MFI 9739
% Max
ROS
Unstained Ctrl.
Non-activated
α-CD3 + α-CD28
α-CD3 + α-CD46
I
IFN-γ (%, normalized to untreated condition)
NA
α-CD3
α-CD3+ α-CD28
α-CD3+ α-CD46
Media
ROS inhibitor
C5aR1/C5aR2 antagonist
C5aR1/C5aR2 antagonist + ROS inhibitor
J
MFI 8012
MFI 12122
% Max
ROS
Unstained Ctrl.
α-CD3 + α-CD46
α-CD3 + α-CD46 + C5aR1/C5aR2 antagonist
MFI 16046
MFI 8446
% Max
ROS
Unstained Ctrl.
Ctrl. siRNA; α-CD3 + α-CD46
C5aR1 siRNA; α-CD3 + α-CD46

Fig. 4

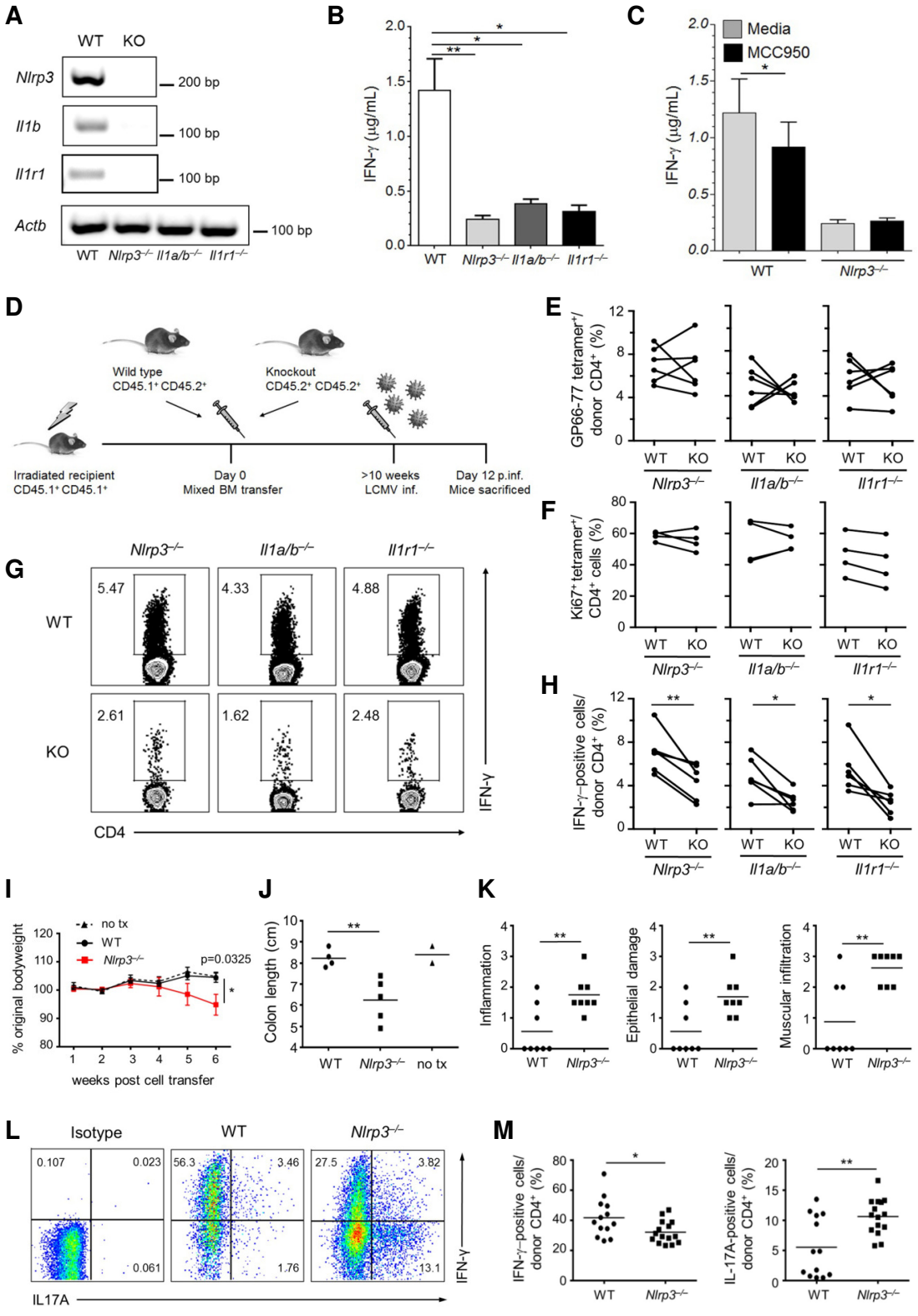
A
WT KO
Nlrp3
Il1b
Il1r1
Actb
200 bp
100 bp
100 bp
100 bp
WT Nlrp3−/− Il1a/b−/− Il1r1−/−
B
IFN-γ (μg/mL)
WT Nlrp3−/− Il1a/b−/− Il1r1−/−
C
Media
MCC950
IFN-γ (μg/mL)
WT Nlrp3−/−
D
Wild type CD45.1+ CD45.2+
Knockout CD45.2+ CD45.2+
Irradiated recipient CD45.1+ CD45.1+
Day 0 Mixed BM transfer
>10 weeks LCMV inf.
Day 12 p.inf. Mice sacrificed
E
GP66-77 tetramer+/ donor CD4+ (%)
WT KO
Nlrp3−/− Il1a/b−/− Il1r1−/−
F
Ki67+tetramer+/ CD4+ cells (%)
G
Nlrp3−/− Il1a/b−/− Il1r1−/−
WT
KO
5.47
4.33
4.88
2.61
1.62
2.48
CD4
IFN-γ
H
IFN-γ–positive cells/ donor CD4+ (%)
I
no tx
WT
Nlrp3−/−
p=0.0325
% original bodyweight
weeks post cell transfer
J
Colon length (cm)
WT Nlrp3−/− no tx
K
Inflammation
Epithelial damage
Muscular infiltration
WT Nlrp3−/−
L
Isotype
WT
Nlrp3−/−
0.107
0.023
0.061
56.3
3.46
1.76
27.5
3.82
13.1
IL17A
IFN-γ
M
IFN-γ–positive cells/ donor CD4+ (%)
IL-17A-positive cells/ donor CD4+ (%)
WT Nlrp3−/−

Supplementary Materials for

Intrinsic NLRP3 inflammasome activity is critical for normal adaptive immunity via regulation of IFN-γ in $CD4^+$ T cells

Giuseppina Arbore, Erin E. West, Rosanne Spolski, Avril A. B. Robertson, Andreas Klos, Claudia Rheinheimer, Pavel Dutow, Trent M. Woodruff, Zu Xi Yu, Luke A. O'Neill, Rebecca C. Coll, Alan Sher, Warren J. Leonard, Jörg Köhl Pete. Monk, Matthew A. Cooper, Matthew Arno, Behdad Afzali, Helen J. Lachmann, Andrew Cope, Katrin D. Mayer-Barber, Claudia Kemper

correspondence to: claudia.kemper@kcl.ac.uk

This PDF file includes:

Materials and Methods

Healthy donors and patients

Blood samples were obtained with ethical and institutional approvals (Wandsworth Research Ethics Committee, REC number 09/H0803/154). T cells were purified blood samples from healthy volunteers after informed consent. Fourteen adult patients with cryopyrin-associated periodic syndrome (CAPS) were recruited at the National Amyloidosis Centre, University College London (Ethical approval REC reference number 06/Q0501/42) with key information on the patients summarized in Table S3. In all experiments that involved T cells from CAPS patients, T cells from age- and sex-matched healthy volunteers were used as controls.

Mice used in the study

All mice used in this study are on a C57BL/6 background (with the exception of the GvHD experiment, were Balb/c mice were used). Wild type and *Il1r1*$^{-/-}$mice were purchased from Jackson Laboratories and subsequently backrossed to B6 for 10 generations at the NIH (Bar Harbor, ME). The *C5ar2*$^{-/-}$ (human gene symbol GPR77, and *gpr77*$^{-/-}$ mice) mice were previously described (*12*), *Nlrp*3$^{-/-}$ animals were provided by Vishwa Dixit of Genentech and mice deficient in *Il1a* and *Il1b* (*Il1a/Il1b*$^{-/-}$ animals) were kindly provided by Y. Iwakura (Tokyo University) (*51*). The C57BL/10 RAG2$^{-/-}$ mice were obtained from Taconic. All animals were maintained in AALAC-accredited BSL2 or BSL3 facilities at the NIH or FDA and experiments performed in compliance with an animal study proposal approved by the NIAID or FDA Animal Care and Use Committee.

Antibodies, proteins, agonists and antagonists

Cell-stimulating mAbs to human CD4^{+} T cells were bought from BD Biosciences, San Diego, CA (anti-hCD28, CD28.2), purified from a specific hybridoma (anti-hCD3; OKT-3) or generated in-house (anti-CD46; TRA-2-10) (*52*). Mouse T cells were activated with anti-CD3 (145-2C11) and anti-CD28 (37.51) from Bio X Cell (West Lebanon, NH). The anti-human/mouse NLRP3 (ab4207), anti-human C5 (ab66850) and C5a (ab11878), anti-human/mouse IL1-β (ab9722) and anti-human β-actin (ab8226) antibodies were purchased from Abcam (Cambridge, UK). The anti-human C5a antibody was also biotinylated in house using the APEX™ Biotin-XX Antibody Labeling Kit (Life Technologies Ltd, Paisley, UK). Alternative antibodies to human/mouse NLRP3/NALP3 (Clone 768319) and human/mouse IL-1β (3A6, used for Western blotting and FACS experiments) were purchased from R&D Systems (Minneapolis, MN) and Cell Signalling Technology (Beverly, MA), respectively. Additional antibodies used include anti-human NLRP3/NALP3 (AG-20B-0014-C100) and ASC (AL177) from Adipogen (Liestal, Switerland), anti-hC5aR1 (sc-53795) and anti-hNLRP3 (sc-34408) from Santa Cruz (Dallas, TX), anti-hC5aR2 (ID9-M12) and anti-hCD45RA from Biolegend, anti-hIL-1β (12-7018-81) and anti-hCD4 from eBioscience (San Diego, CA), anti-hC5aR1 (MCA2059; AbD Serotec, Oxford, UK), anti-hC5aR2 (PA1-41397; Thermo Scientific (Leicestershire, UK)), and anti-hcaspase-1 (3019-100; Biovision (Milpitas, CA)). The antibodies recognizing anti-human-CD25, CD45RA (555488), and CD45RO (559865) were purchased from BD Biosciences. The following mouse antibodies were purchased from Biolegend: Mouse Trustain (Fc-Block), anti-CD44 FITC, PE-cy7 or BV421, anti-mouse IFN-γ PE, anti-mouse CD4 (APC-cy7, BV 421 or BV605), anti-mouse CD45.1 FITC and CD45.2 PerCP, anti-mouse CD45RB FITC, anti-mouse CD25 APC. Anti-mouse/human Ki67 was purchased from BD Biosciences. The secondary antibodies anti-rabbit IgG H+L chain Alexa Fluor 594 (ab150076), anti-goat IgG H+L chain PE (ab7004) and anti-goat IgG H+L chain Alexa Fluor 488 (ab150129) were from Abcam, while anti-mouse IgG Alexa Fluor 488 (A11001), anti-rabbit IgG H+L chain Alexa Fluor 594 (A11037) and anti-rat IgG H+L chain Alexa Fluor 488 (A11006) were obtained from Molecular Probes/Life Sciences (Paisley, UK). APC streptavidin was purchased from Biolegend.

Recombinant active human IL-1β was bought from Abcam and used at 20 ng/ml in cultures, recombinant human IL18BPa (Sino Biologicals Inc.) was used at 50 μM, human IL-2 was provided by C. Pham (Washington University in Saint Louis, MO) and lipopolysaccharide (LPS) was purchased from Sigma Aldrich (Saint Louis, MO). Recombinant C5 and C5adesArg were purchased from CompTech (Tyler, TX). The specific C5aR1 antagonist (PMX53) (*17*) was provided by T. Woodruff (University of Queensland, AU) and used at 10 μM, the C5aR1/C5aR2 double antagonist a gift from J. Köhl (University of Lübeck, Germany) (*18*) and used at 7 μM, and the specific C5aR2 agonist (RHYPYWR) was generated by T. Woodruff and P. Monk (Sheffield University, UK) (*19*) and used at 100 μM. The specific NLRP3 inhibitor MCC950 (*36*) was used at 10 μM, the specific caspase-1 inhibitor Z-YVAD-FMK (Abcam) was used at 20 μM and the reactive oxygen species (ROS) inhibitor Diphenyleneiodonium (DPI) (Sigma Aldrich) was added at 750 nM. In all experiments, cells were incubated in media for 15 minutes including the compound of choice (incubation with the corresponding vehicle buffer was used as control) before activation and culture.

Cell isolation and activation

Human cells: $CD4^+$ T cells and monocytes were isolated from blood as previously published using the MACS Human $CD4^+$ Positive T cell Isolation Kit or the MACS Human $CD14^+$ Cell Positive Isolation Kit (both Miltenyi, Biotech Ltd, Bisley, UK), respectively (*7*). Purity of bead-isolated T lymphocyte fractions was typically > 98% and for monocytes > 95%. For (naïve and memory) $CD4^+$ T cell sorting, cells were stained with appropriate antibodies (naïve cells: $CD4^+$, $CD45RA^+$, $CD45RO^-$, $CD25^-$ and memory cells: $CD4^+$, $CD45RA^-$, $CD45RO^+$, $CD25^-$) and sorted with a BD FACSAria™ II Cell Sorter (KCL Flow Core facility). $CD4^+$ T cells were activated in 48-well culture plates (2.5 – 3.0 x 10^5 cells/well) coated with mAbs to CD3, CD28 or CD46 (2.0 μg/ml PBS each) and addition of 25 U/ml rhIL-2, thus, under non-skewing conditions. Monocytes were activated in 24-well plates (2.5 – 5.0 x 10^5 cells/well) by addition of LPS (50 ng/ml). Cell viability was monitored by using either propidium iodide (BD Biosciences) or the LIVE/DEAD Cell Viability Assay (Life Technologies).

Mouse cells: Single cell suspensions of spleen cells were generated and red blood cells lysed using ACK lysis buffer (Life Technologies). $CD4^+$ T cells were isolated by negative selection using the Stem Cell Technologies EasySep™ Mouse $CD4^+$ T Cell Isolation Kit (Tukwila, WA). To obtain pure $CD4^+$ T cell populations, $CD4^+$ cells were sorted using a FACS Aria (BD Biosciences) based on $CD4^+CD45.2^+$ staining and to separate naïve versus memory $CD4^+$ T lymphocytes. T cells were sort-separated based on $CD4^+$ $CD44^+$ (memory) and $CD4^+$ $CD44^-$ (naïve) stainings. For *in vitro* T cell activation, 48- or 96-well plates were coated with 2 ug/ml anti-CD3 overnight at 4°C and $CD4^+$ T cells (0.5 – 1.0 x 10^6 per well of 48-well plates or 0.2 x 10^6 per well of 96-well plates) were added to the appropriate wells. One ug/ml of anti-CD28 was added to the media to provide co-stimulation.

Lymphocytic choriomeningitis virus (LCMV) infection in mice

Preparation of mixed bone marrow (BM) chimeric mice: B6.SJL (CD45.1,1) mice were lethally irradiated (950 rad) and reconstituted with a total of 10^7 donor BM cells from C57BL/6 CD45.1,2 wild-type (WT) mice mixed at equal parts with BM cells from CD45.2,2 mice deficient (KO) in either *Nlrp3-/-*, *Il1r1-/-*, or *Il1a/Ilb-/-*. Mice were allowed to reconstitute for 10 weeks before infection with LCMV.

LCMV infection and assessment of antigen-specific $CD4^+$ T cell response: Ten weeks post-reconstitution, the mice were infected with 10^5 pfu of LCMV-Armstrong intraperitoneally. On day 12 post-infection, the mice were euthanized and the spleens removed for processing. For *ex vivo* cytokine staining of mouse cells after LCMV infection, cells were incubated with 1 ug/ml of LCMV GP61-80 peptide in the presence of monensin and brefeldin for 5 hours at 37 ^oC. Staining for LCMV-specific $CD4^+$ T cells was performed using an APC-labeled $1A^b$ LCMV GP66-77 tetramer (NIH tetramer core facility) as described previously *(53)*. Data were acquired with a FACS Calibur, Fortessa LSRIII or FACS Aria cytometer (BD Biosciences) and analyzed with FlowJo 10.0.8 software (Ashland, OR).

Induction of colitis and colon cell isolation

Splenic $CD4^+$ T cells were isolated from C57BL/6 or *Nlpr3*$^{-/-}$ mice using a negative selection CD4 T cell enrichment kit (Stemcell tech), were stained with anti-CD45RB FITC, anti-CD25APC and anti-CD4 BV421, and sorted on a FACS Aria (BD biosciences) for $CD4^+$ $CD25^-CD45RB^{hi}$ (brightest 35%) cells. 2 x 10^5 of WT or *Nlpr3*$^{-/-}$ cells were injected i.p. into age and sex matched C57BL/10 $RAG2^{-/-}$ mice. The mice were sacrificed when symptoms of clinical disease (5-10% weight loss of original bodyweight and/or diarrhea) were observed in at least one group, approximately 6-11 weeks after adoptive transfer. Colon lamina propria cells were isolated as described previously (*54*), with the additional step of further purifying the cells over a 44% and 67% Percoll gradient to enrich for the mononuclear cells.

Scoring of intestinal inflammation

Samples of the proximal, mid and distal colon were excised after feces were flushed from the colons, placed into 3.7% formaldehyde solution, and then paraffin embedded. Cross-sectional sections were cut and stained with haematoxylin and eosin (H&E). Colon pathology scores were based on severity of mononuclear cell inflammation, intestinal wall thickening, including infiltration to the muscularis, and epithelial damage, including edema, degeneration, and necrosis on a graded scale where 0 = normal, 0.5 = very mild, 1 = mild, 2 = moderate, 3 = severe. Samples were scored blinded by a pathologist from the NIH Pathology Score.

Induction of graft versus host disease (GvHD)

Balb/c mice were lethally irradiated with 900cGy (two doses of 450cGy 3 hours apart) on day -1. C57BL/6 WT bone marrow was depleted of T cells using the CD90.2 Positive Selection Kit (Stemcell tech) and 5 x 10^6 cells were transferred on the following day (day 0) alone (control), or in addition to 1 x 10^6 WT B6 or *Nlpr3*$^{-/-}$ naïve CD4$^+$ T cells isolated with the Negative Selection Naïve CD4 T Cell Kit (Stemcell tech). Mice were sacrificed upon clinical symptoms of disease (diarrhea and weight loss) on day 12 post cell transfer.

Detection of active caspase-1 and reactive oxygen species (ROS)

Generation of cleaved and active caspase-1 in cells was monitored by Western blotting for appropriate active fragment generation and by using the Green FLICA Caspase-1 Assay Kit (ImmunoChemistry Technologies, Bloomington, MN) according to the manufacturer's protocol with subsequent FACS analysis. ROS staining was performed by incubating cells to be assayed in 17 µg/ml dihydrorhodamine (DHR) 123 diluted in Hank's balanced salt solution with 10 mM HEPES (all from Sigma Aldrich) for 15 minutes at 37 °C. Data were acquired on a FACS Calibur or Fortessa LSRIII cytometer (BD Biosciences) and analyzed with FlowJo software.

Confocal microscopy

Cells were fixed and permeabilized using the Cytofix/Cytoperm Kit (BD Biosciences) and stained with the indicated primary antibodies overnight and with secondary antibodies 30 min at 4 °C. Cells were mounted using VECTASHIELD media with DAPI (Vector Laboratories Ltd., Burlingame, CA) and images were acquired with a Nikon A1R confocal microscope (Nikon Imaging Centre, King's College London, London, UK) and analyzed using NIS Elements (Nikon, Surrey, UK) and ImageJ software (National Institute of Health, MD).

Binding studies with recombinant human ^{125}I-C5a

CD4$^+$ T cells from healthy donors were left non-activated or activated for 4 hours with immobilized antibodies to CD3 and CD46 and then incubated for 2 hours at 4 °C (1 x 10^7 cells/ml) with 10 µl of 0.1 nM ^{125}I-rhC5a (Perkin Elmer, Boston, MA, USA) and either 400 nM non-labelled rhC5a in HAG-CM buffer (1 mM $CaCl_2$, 1 mM $MgCl_2$, 0.25% bovine serum albumin, 0.5 mM glucose, pH 7.4) or buffer without rhC5a addition. Cells were vacuum-transferred onto 96-well MultiScreen-HV filter plates (MAHVN4510; Millipore/Merck, Darmstadt, Germany), non-bound ^{125}I-rhC5a removed by washing and cell-bound ^{125}I-rhC5a detected on the filter membranes by ^{125}I using a Packard Cobra II Gamma Counter (Perkin Elmer, Schwadorf, Austria). For binding controls, human embryonic kidney (HEK 293) cells (ATCC CRL 1573) were stably transfected with the pQCXIN vector expressing hC5aR1 or hC5aR2 (leading to expression of >1 Mio. of the respective C5aR/cell) or with the 'empty' vector as control (*55*) (these cell lines also served as specificity controls for the anti-C5a receptor antibodies used in this study). In order to get comparable low cpm-values as observed with purified T cells, only 5 x 10^4 cells/ml of C5aR1- or C5aR2-expressing HEK cells were applied. They were diluted in buffer containing 'no-C5aR-expressing control' cells. The constant higher number of cells (5 x 10^5 HEK cells/ml in the 30µl volume later used in the binding assay) permitted repetitive washing without cell-loss and ensured identical non-specific binding in all samples containing the same cell type. C5aR1- , C5aR2-expressing or control HEK 293 cells were incubated for 1 hour with or without 100 nM of non-labelled rhC5a, washed thoroughly and then incubated for additional 2 hours with 10 µl of 0.1 nM ^{125}I-rhC5a. After removal of non-bound rhC5a, binding of ^{125}I-C5a to the respective HEK 293 cell lines was determined by measuring gamma radioactivity. To exclude C5a-induced C5aR-internalization during all binding studies all steps in the binding experiments were performed at 4°C and HEK 293 cells were additionally pre-incubated 15 minutes at 37°C with 0.1% NaAcid and 21 µg/ml Cytochalasin B, and then cooled on ice for 5 minutes before their incubation with rhC5a.

Cytokine measurements

Cytokine production by cells in culture was quantified from cell supernatants using either the human or mouse Th1/Th2/Th17 Cytometric Bead Array (BD Bioscience) or via intracellular cytokine staining after treated for 4 hours with 50 ng/ml PMA, 1 µg/ml ionomycin (both Sigma Aldrich) and 1 x Golgi Plug (BD Biosciences). Secreted human IL-1β and IL-18 were measured using the Human IL-1β/IL-1F2 DuoSet Kit or the Human IL-18/IL-1F4 Elisa kit (R&D Systems and eBiosciences, respectively) in combination with SIGMAFAST^{TM} OPD tablets (Sigma Aldrich) as substrate for detection.

RNA extraction, RT-PCR and quantitative RT-PCR

RNA was extracted utilizing the RNeasy Mini Kit including DNAse digestion and DNA cleanup (Qiagen, Limburg, The Netherlands) and reverse transcription performed with the One Step RT-PCR (Qiagen). For quantitative PCR, RNA was reverse-transcribed with 2.5 μM random hexamers, 1 mM dNTPs, 40 U RiboLock RNAse inhibitor and 400 U RevertAid H Minus Reverse Transcriptase (Thermo Scientific). Quantitative-PCR was performed using KI-Q Hot Start Sybr Green Mix (Sigma Aldrich), with 150 pmol forward and reverse primers and data acquired on the CFX96 Touch™ Real-Time PCR Detection System (Bio-Rad, Hertfordshire, UK). Primer sequences are listed in Table S5.

RNA silencing

SiRNA targeting human C5AR1 mRNA and control scrambled siRNA were purchased from Origene (Rockville, MD) and delivered at a final concentration of 15 nM (mixture of 3 different C5aR1 siRNA used at 5nM each or scramble control at 15nM) into primary human $CD4^+$ T cells by transfection with Lipofectamine RNAiMAX (Life Technologies, Paisley, UK) following the manufacturer's instructions. *C5AR1* mRNA level reduction was consistently about 30 %.

Microarray data generation and analysis

Transcriptome profiling was performed by the KCL Genomic Centre (London, UK) utilizing human exon 1.0 ST arrays (Affymetrix, High Wycombe, UK) on $CD4^+$ T cells isolated from three different healthy donors that were left either non-activated or were activated with antibodies to CD3 and CD46 for 2 hours in the absence or presence of the C5aR1/C5aR2 antagonist. Expression data were analyzed using Partek Genomics Suite (Partek Inc., St Louis, USA) version 6.6 and Gene Set Enrichment Analysis, GSEA (*56*) (Broad Institute of MIT and Harvard, USA) with a normalized enrichment score of 1.8 to derive normalized enrichment score (NES), nominal *p*-value and FDR q-value. Microarray datasets were used in conjunction with the Qiagen-generated inflammasome gene set (Qiagen Sciences Inc, USA) (84 members). Heatmaps for the leading edge subset were drawn with Partek genomics suite. Table S1 shows the normalized read values from microarrays for Fig. 2A and B. The list of annotated genes differentially regulated by the C5aR1/C5aR2 double antagonist (fig. S2) is given in Table S2.

Statistical analysis

Analyses were performed with GraphPad Prism (La Jolla, CA). Data are presented as mean ± SEM and compared using either paired t-tests with Bonferroni correction for multiple comparisons, one-way or two-way ANOVA with a Tukey multiple comparison *post hoc* test, as appropriate. Correlation analysis (Fig. 2J ans S2L) was performed with Spearman correlation test. P values < 0.05 denote statistical significance.

Figure legends

Fig. S1. Autocrine activation of C5a receptors regulates IFN-γ production by human CD4$^+$ T cells. (A) C5aR1 and C5aR2 Western blot analyses on cytoplasmic (Cyt.) and membrane (Mem.) fractions of resting human CD4$^+$ cells (representative of n=3). **(B** and **C)** Representative flow cytometry histograms for intracellular staining **(B)** and immunoblot with cytoplasmic (Cyt.) and membrane (Mem.) fractions **(C)** on C5aR1 and C5aR2 in HEK293 cells (HEK) transfected with a vector expressing either C5aR1, or C5aR2, or an empty control vector (Ctrl. Vec.). **(D)** Binding of radioactively-labelled ^{125}I-C5a to HEK293 cells expressing either C5aR1, C5aR2 or no C5a receptor in the absence or presence of non-labelled 'cold' C5a as competitor (n=3). **(E)** IFN-γ production in CD4$^+$ T cells activated for 36 hours with α-CD3 + α-CD46 in presence of increasing concentrations of exogenous C5a or C5adesArg (n=3), with significance assessed between untreated cells (0 ng/mL C5a or C5adesArg) and cells treated with indicated amounts of either C5a or C5adesArg. **(F)** IL-17 and IL-4 production by non-activated (NA) and activated (36 hours) CD4$^+$ T cells in the absence or presence of either a C5aR1/C5aR2 double receptor antagonist (n=9), a C5aR2 agonist (n=8) or a C5aR1 antagonist (n=7). **(G)** Cell viability of T cells either resting or activated for 36 hours as indicated in the absence or presence of the C5aR1/C5aR2 double antagonist or C5aR2 agonist (n=2). **(H)** Reduction of *C5AR1* mRNA levels in T cells transfected with either a C5AR1-specific siRNA or a scrambled control siRNA (Ctrl. siRNA) 48 hours post transfection. Left panel shows a representative mRNA expression sample and the right sample statistically significant reduction in *C5AR1* mRNA expression in C5AR1-specific siRNA-treated CD4$^+$ T cells (n=6). Error bar graphs represent mean ± SEM. **p* <0.05, ***p* <0.01, ****p* <0.001.

Supp. Fig. 2 NLRP3 inflammasome activation occurs in CD4$^+$ T cells and enhances IFN-γ production. (A) Volcano plot showing transcripts differentially regulated in CD4$^+$ T cells from 3 donors after α-CD3 + α-CD46 activation (2 hours) with or without addition of the C5aR1/C5aR2 antagonist to cultures. **(B)** Quantitative RT-PCR to measure *NLRP3* and *IL1B* mRNA in non-activated (NA) or α-CD3 + α-CD46 activated human CD4$^+$ T cells at 36 hours post activation (n=3, expression normalized to *ACTB*). (**C** and **D**) Representative NLRP3 expression assessed by flow cytometry (**C**) and by immunofluorescence (**D**) in non-activated naïve and memory human CD4$^+$ T cells (n=3). **(E** and **F)** Representative caspase-1 and IL-1β immunoblot analyses (with lower arrows depicting the activated protein forms), performed on resting and α-CD3 + α-CD46 activated CD4$^+$ T cells (36 hours) and resting and LPS activated monocytes (50 ng/ml, 18 hours) (representative of n=4) with densitometric analyses on activated caspase-1 and IL-1β in T cells. The corresponding quantitative data shown below the immunoblots do not depict absolute amounts of proteins in monocytes versus T cells. They depict the ratio (percentage) of non-cleaved (non-activated) versus cleaved (activated) protein in either T cells or in monocytes. **(G)** IL-17 and IL-4 secretion in CD4$^+$ cells non-activated (NA) or activated as indicated with or without the NLRP3 inhibitor MCC950 at 36 hours post activation (n=7). **(H)** Cell viability of CD4$^+$ cells either resting or activated for 36 hours as indicated in the absence or presence of the NLRP3-specific inhibitor MCC950 (n=2). **(I)** IL-1β secretion by resting (NA) and activated CD4$^+$ T cells (36 hours) with or without addition of the caspase-1 inhibitor Z-YVAD-FMK (n=4). (**J**) IL-18 production in α-CD3 + α-CD46 activated CD4$^+$ T cells (36 hours) from three HDs (left panel) and IFN-γ production in CD4$^+$ T cells from HDs 1 and 2 by T cells activated with α-CD3 + α-CD46 for 36 hours in full media and for 72 hours in

serum free media, in the presence of 50 μM of rIL18BP (right panel). **(K)** IL-1β from $CD4^+$ T cells activated with α-CD3 + α-CD46 for 36 hours from four healthy donors (HD1-4) and 7 patients with CAPS (P1-7). **(L)** Percentages of naïve and memory $CD4^+$ T cell subpopulations in the blood of a second cohort of CAPS patients P8 to P14 and of three sex- and age-matched healthy donors (HD5-HD7). **(M)** Correlation between active caspase-1 and IL-1β production in T cells from patients P8-P14 upon CD3 + CD46 activation (Spearman correlation analysis). Error bar graphs represent mean ± SEM. *p <0.05, **p <0.01.

Supp. Fig. 3. C5a receptors regulate NLRP3 activation to modulate IFN-γ responses. (**A** and **B**) Quantitative RT-PCR to measure *NLRP3* **(A)** and *IL1B* mRNA **(B)** in resting or α-CD3 + α-CD46 activated (2 hours) human $CD4^+$ T cells in the absence or presence of the C5aR1/C5aR2 antagonist with the respective corresponding bar graphs (panel below) showing relative expression in activated versus non-activated cells with or without C5aR1/C5aR2 antagonist-treated T cells (n=3, expression normalized on *ACTB*). (**C**) IL-17 and IL-4 production in resting or activated T cells in presence or absence of MCC950 and/or the C5aR1/C5aR2 double antagonist at 36 hours (n=4). (**D**) NLRP3 expression in $CD4^+$ T lymphocytes either left non-activated or activated with α-CD3, α-CD3 + α-CD28 or α-CD3 + α-CD46 for 36 hours with or without addition of the C5aR1/C5aR2 antagonist (upper row) or the C5aR2 agonist (lower row) to cultures (data representative of n=3). **(E)** NLRP3 expression after α-CD3 + α-CD46 activation (36 hours) in T cells transfected with either C5aR1-specific siRNA or scrambled control (Ctrl.) siRNA (data representative of n=3). (**F**) IL-17 and IL-4 secretion (shown as % normalized to respective untreated conditions) from $CD4^+$ T cells left non-activated (NA) or activated as indicated with or without a specific ROS inhibitor and/or the C5aR1/C5aR2 antagonist at 36 hours post activation (n=3). Error bar graphs represent mean ± SEM. *p <0.05, **p <0.01, ***p <0.001.

Supp. Fig. 4 NLRP3 function in $CD4^+$ T cells is required for optimal IFN-γ response *in vivo*. (**A**) Representative immunofluorescence analysis for NLRP3 and IL-1β protein expression on $CD4^+$ T cells isolated from wild type (WT), *Nlrp3*$^{-/-}$ and combined *Il1a*$^{-/-}$ and *Il1b*$^{-/-}$ (*Il1a/b*$^{-/-}$) mice. **(B)** Percentages of naïve and memory $CD4^+$ T cells isolated from the spleen of unchallenged wild type (WT) and *Nlrp3*$^{-/-}$, combined *Il1a*$^{-/-}$ and *Il1b*$^{-/-}$ (*Il1a/b*$^{-/-}$), and *Il1r1*$^{-/-}$ mice (n=3). **(C)** Cell viability of sorted $CD4^+$ T cells from WT and knock out mice 96 hours post CD3 + CD28 activation (n=3). **(D)** IL-10, IL-4 and IL-17 secretion from $CD4^+$ T cells isolated from WT and knock out mice activated 96 hours with antibodies to CD3 and CD28 (n=3). **(E)** Cell viability of sorted $CD4^+$ T cells from WT and *Nlrp3*$^{-/-}$ mice assessed with or without MCC950 addition (right panel) during activation (96 hours post α-CD3 + α-CD28 activation, n=4). (**F**) IL-10, IL-4 and IL-17 secretion from $CD4^+$ T cells activated 96 hours with antibodies to CD3 and CD28 from WT and *Nlrp3*$^{-/-}$mice with or without addition of MCC950 (n=4). **(G and H)** IFN-γ, IL-10, IL-4 and IL-17 secretion from sorted naïve **(G)** and memory **(H)** $CD4^+$ T cells from WT, *Nlrp3*$^{-/-}$, *Il1a/b*$^{-/-}$, and *Il1r1*$^{-/-}$ mice 96 hours post α-CD3 + α-CD28 activation (n=3). Error bar graphs represent mean ± SEM. *p <0.05.

Supp. Fig. 5 Lack of intrinsic NLRP3 inflammasome function in $CD4^+$ T cells impacts on GvHD disease. (**A-D**) Disease scores and Th1 and Th17 T cell populations. T cell-depleted C57BL/6 bone marrow was transferred into lethally irradiated BALB/c mice alone (control group), or with the addition of 1 x 10^6 naïve $CD4^+$ T cell from either

C57BL/6 or *Nlpr3*$^{-/-}$ mice. (**A**) Colon length at study endpoint (12 days post-cell transfer). (**B-D**) Intracellular IFN-γ and IL-17A staining of mesenteric lymph node CD4$^+$ T cells at the study endpoint after overnight α-CD3 and α-CD28 stimulation and brefeldin A and monensin addition for 5 hours (Gated on live CD4$^+$ Thy1.2$^+$ C57BL/6 (H-2K^{d}D^{d+}) T cells). Percent (**B**) and mean fluorescence intensity (MFI) of IFN-γ$^+$ cells (**C**) and percent IL-17A$^+$ cells (**D**). For (**A-D**) n=4 WT, 5 KO, 2 controls. (**E**) *In vitro* cytokine production of CD4$^+$ T cells from wild type and *C5ar2*$^{-/-}$ mice with or without addition of MCC950 at 48 hours post α-CD3 + α-CD28 activation. Error bar graphs represent mean ± SEM. **p* <0.05, ***p* <0.01, ****p* <0.001.

Supp. Fig. 6 The C5aR2-NLRP3-IL-1β axis may regulate 'IL-10 switching' in human Th1 cells. (A) Suggested model of complement-regulated inflammasome activation during Th1 responses: TCR stimulation together with CD46 (via autocrine C3b generation, not shown) engagement triggers intracellular C5 activation and C5a generation. Subsequent intracellular C5aR1 engagement mediates ROS production and NLRP3 assembly which in turn induces caspase-1-mediated IL-1β maturation. Autocrine IL-1β function promotes IFN-γ production and Th1 induction but restricts 'IL-10 switching' (at least in human CD4$^+$ T cells). C5aR2 cell surface activation by secreted C5a (or C5adesArg) negatively controls these events (either via direct inhibition of C5aR1 activation and/or other yet undefined mechanisms) thereby allowing for IL-10 co-induction during Th1 contraction. It is currently unclear whether intracellular C5aR2 activation occurs and what the potential role of such stimulation could be. **(B)** IFN-γ to IL-10 ratio in α-CD3 + α-CD28 or α-CD3 + α-CD46 activated (36 hours) CD4$^+$ T cells in the absence or presence of either a C5aR1/C5aR2 double receptor antagonist (n=9), a C5aR2 agonist (n=8) or a C5aR1 antagonist (n=7). **(C)** IL-10 production by resting and activated CD4$^+$ T cells, in presence or absence of MCC950 and/or rhIL-1β measured at 36 hours post activation (n=3). **(D)** IL-10 secretion at 36 hours post indicated activation by CD4$^+$ cells from the patients with CAPS P8-P14 and seven sex- and age-matched healthy donors (HD5-11) with data represented as mean ± SEM. Error bar graphs represent mean ± SEM. **p* <0.05, ***p* <0.01.

Table S1.

Normalized read values from microarrays for Fig. 2A and B

Table is provided in Other Supplementary Material as an Excel file.

ID	p-value	Fold change
C15orf48	0.0118739	2.08331
C3orf14	0.0327513	2.13952
CXCL2	0.0330927	5.59906
DDX60	0.00208813	2.38253
DTX3L	0.0101958	2.02692
EIF2AK2	0.00659247	3.45509
EREG	0.00093681	2.50735
FAM45B	0.035722	2.16729
HERC6	0.00197424	2.8311
HSH2D	0.0219705	2.13182
IFI44	0.00790994	2.89407
IFI44L	0.0204978	4.5496
IFIH1	0.00489751	2.63568
IFIT1	0.0250406	3.36767
IFIT3	0.0192085	4.57257
IFIT5	0.00982865	2.10946
IL1A	0.0137544	3.52362
IL1B	0.0053077	2.36807
IL6	0.0145825	3.11426
IL8	0.00751255	3.61565
LAMP3	0.0046064	2.25455
MX1	0.032786	4.21644
NM_001199779 // PSMB2	0.0148295	-2.09297
OAS2	0.010885	4.16812
OR4N2	0.0348681	-2.69263
PARP9	0.0314253	3.3435
PTGS2	0.00566655	3.80875
SAMD9	0.0116602	2.07468
SAMD9L	0.0364514	3.18497
SERPINB2	0.0268882	3.68178
TNFAIP6	0.0045844	2.61021

Table S2.

Genes differentially regulated by the C5aR1/C5aR2 double antagonist
Reported the p-value and the fold change (α-CD3 + α-CD46 + C5aR1/C5aR2 double antagonist vs α-CD3 + α-CD46)

Patient N°	Age/gender	NLRP3 Mutation	Treatment
1	59 y./female	V198M	Canakinumab
2	29 y./female	V198M	Canakinumab
3	45 y./male	T436I	Anakinra
4	53 y./male	mut neg (mosaic c.1699G>A, E567K, in 5.2% of cells)	Anakinra
5	72 y./male	A439V	Canakinumab
6	22 y./male	R260W	Canakinumab
7	16 y./male	R260W	Canakinumab

Table S3.
Details of seven patients (1 to 7) with cryopyrin-associated periodic syndrome (CAPS)

Patient N°	Age/gender	NLRP3 Mutation	Treatment
8	31 y./female	A439V	Canakinumab
9	52 y./female	A439V	Canakinumab
10	29 y./female	A439V	Canakinumab
11	55 y./female	A439V	Canakinumab
12	27 y./female	A439V	Starting canakinumab
13	60 y./female	A439V	Starting canakinumab
14	67 y./female	somatic mosaicism (none in germline)	On anakinra for 3 weeks

Table S4.
Details of seven patients (8 to 14) with cryopyrin-associated periodic syndrome (CAPS) and A439V mutation

Gene	Primer Forward	Primer Reverse
C5AR1	5'-CACTAGGGCCCAGAAGAC-3’	5'-AAGAGTCCCGCTGGAAAAGG-3’
C5AR2	5’-GCTCTTCCTGTATTTTGGGAGGG-3’	5’-GCTGGTGGATTTCTTGCTGTCC-3’
NLRP3	5’-GGCAACACTCTCGGAGACAAG-3’	5’-GCTCTGGCTGGAGGTCAGAA-3’
IL1B	5'-CTCGCCAGTGAAATGATGGCT-3'	5'-GTCGGAGATTCGTAGCTGGAT-3'
ACTB	5'-ACGGCCAGGTCATCACCATTG-3'	5'-AGTTTCGTGGATGCCACAGGAC-3'
Nlrp3	5’-AGCCAGAGTGGAATGACACG-3’	5’-CGTGTAGCGACTGTTGAGGT-3’
Il1b	5’-ATCAACCAACAAGTGATATTCTCCAT-3’	5’-GGGTGTGCCGTCTTTCATTAC-3’
Il1r1	5’-ATGGAAGTCTTGTGTGCCCT-3’	5’-TCCGAAGAAGCTCACGTTGT-3’
Actb	5’-GATGCCCTGAGGCTCTTTTCC-3’	5’-GAGGTCTTTACGGATGTCAACGTCA-3’

Table S5.
Listed primers sequences

Fig. S1

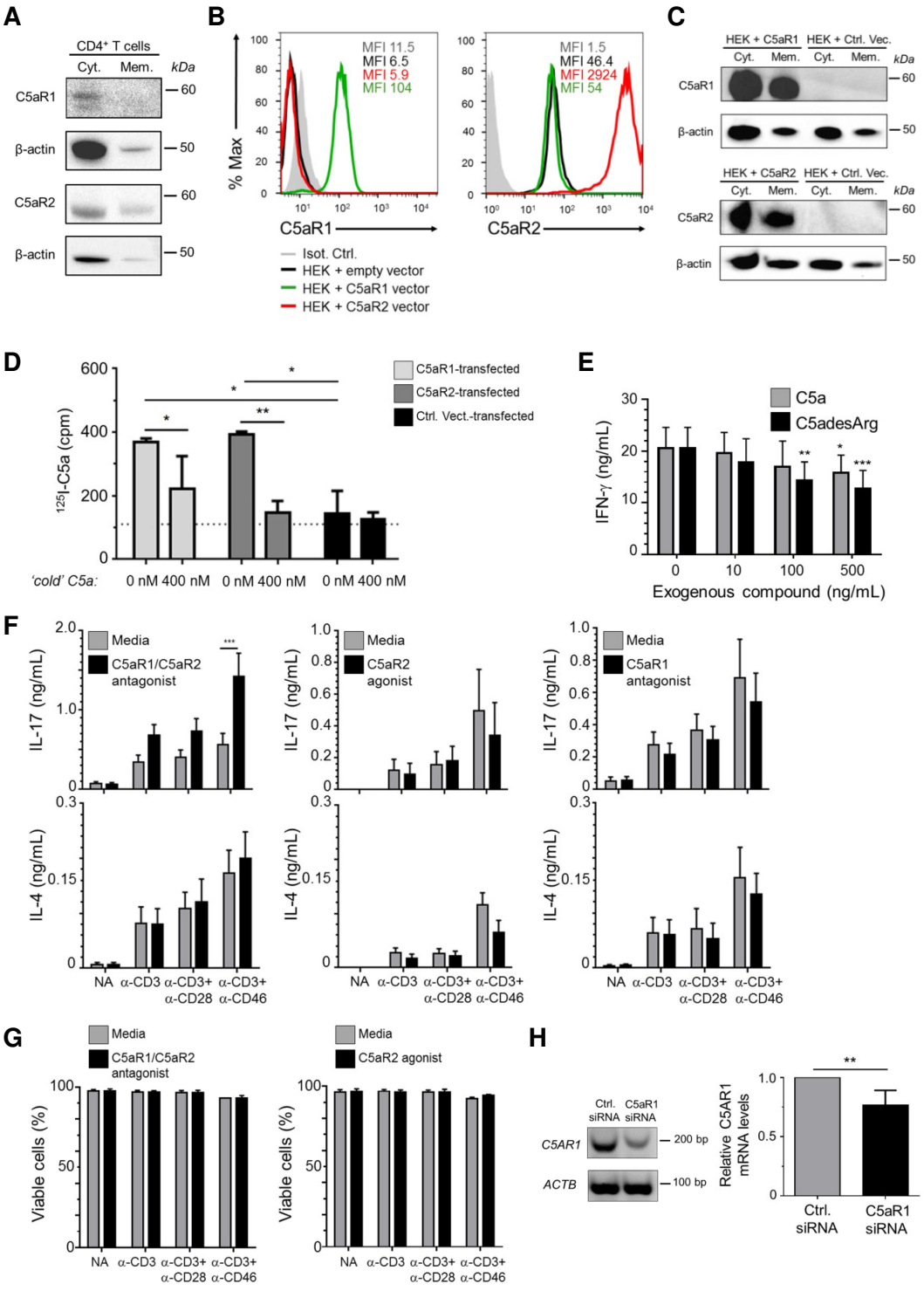
A
CD4+ T cells
Cyt.
Mem.
kDa
C5aR1
β-actin
C5aR2
β-actin
60
50
60
50
B
% Max
MFI 11.5
MFI 6.5
MFI 5.9
MFI 104
MFI 1.5
MFI 46.4
MFI 2924
MFI 54
C5aR1
C5aR2
Isot. Ctrl.
HEK + empty vector
HEK + C5aR1 vector
HEK + C5aR2 vector
C
HEK + C5aR1
HEK + Ctrl. Vec.
HEK + C5aR2
D
125I-C5a (cpm)
C5aR1-transfected
C5aR2-transfected
Ctrl. Vect.-transfected
'cold' C5a:
0 nM 400 nM 0 nM 400 nM 0 nM 400 nM
E
IFN-γ (ng/mL)
C5a
C5adesArg
Exogenous compound (ng/mL)
F
IL-17 (ng/mL)
IL-4 (ng/mL)
Media
C5aR1/C5aR2 antagonist
C5aR2 agonist
C5aR1 antagonist
NA
α-CD3
α-CD3+ α-CD28
α-CD3+ α-CD46
G
Viable cells (%)
Media
C5aR1/C5aR2 antagonist
C5aR2 agonist
H
Ctrl. siRNA
C5aR1 siRNA
C5AR1
ACTB
200 bp
100 bp
Relative C5AR1 mRNA levels

Fig. S2

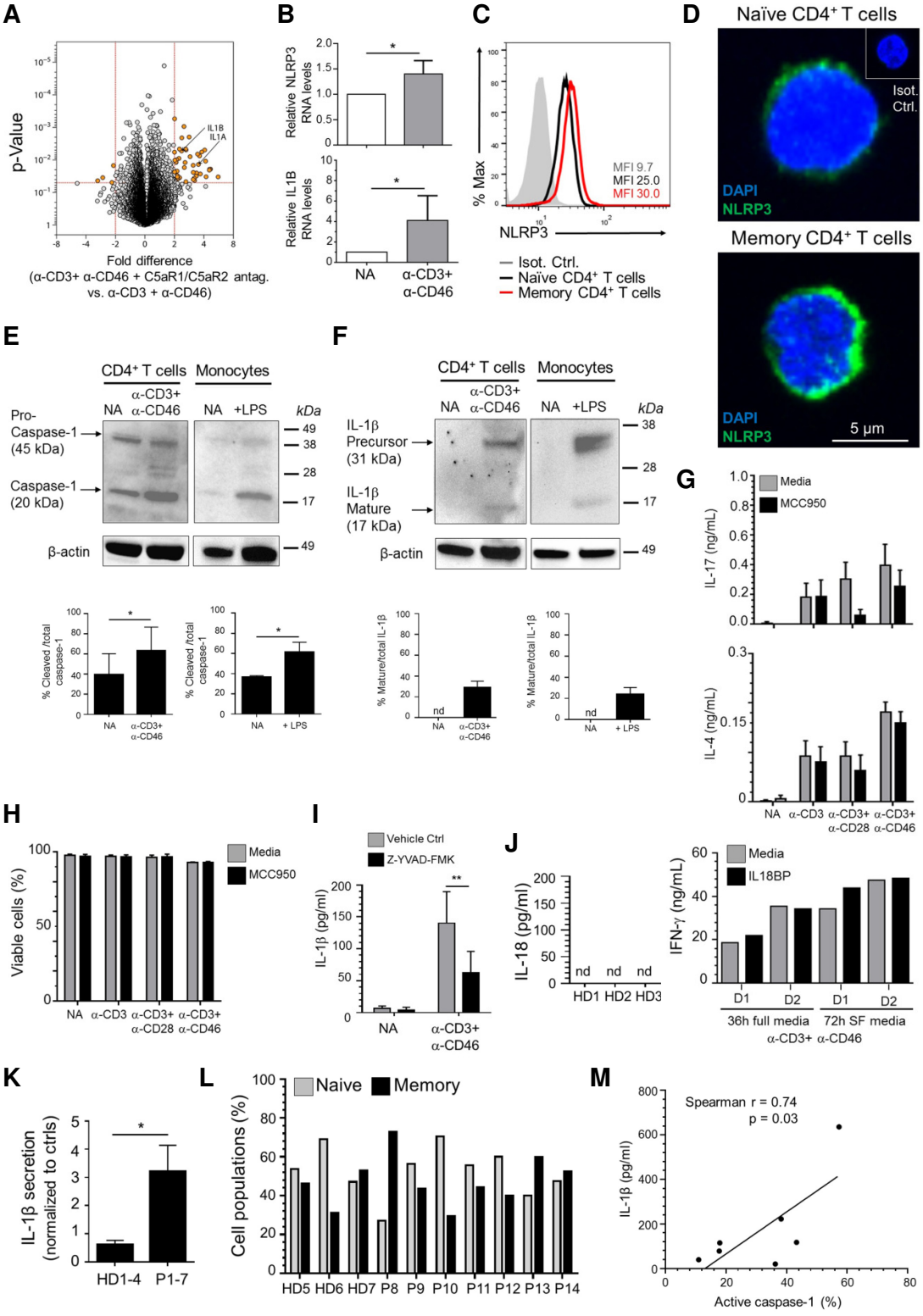
A
p-Value
IL1B
IL1A
Fold difference
(α-CD3+ α-CD46 + C5aR1/C5aR2 antag.
vs. α-CD3 + α-CD46)
B
Relative NLRP3 RNA levels
Relative IL1B RNA levels
NA
α-CD3+ α-CD46
C
% Max
MFI 9.7
MFI 25.0
MFI 30.0
NLRP3
Isot. Ctrl.
Naïve CD4+ T cells
Memory CD4+ T cells
D
Naïve CD4+ T cells
Isot. Ctrl.
DAPI
NLRP3
Memory CD4+ T cells
5 µm
E
CD4+ T cells
Monocytes
α-CD3+ α-CD46
NA
+LPS
kDa
Pro-Caspase-1 (45 kDa)
Caspase-1 (20 kDa)
β-actin
% Cleaved /total caspase-1
F
IL-1β Precursor (31 kDa)
IL-1β Mature (17 kDa)
% Mature/total IL-1β
nd
+ LPS
G
Media
MCC950
IL-17 (ng/mL)
IL-4 (ng/mL)
NA
α-CD3
α-CD3+ α-CD28
α-CD3+ α-CD46
H
Viable cells (%)
I
Vehicle Ctrl
Z-YVAD-FMK
IL-1β (pg/ml)
J
IL-18 (pg/ml)
HD1 HD2 HD3
IFN-γ (ng/mL)
IL18BP
D1
D2
36h full media
72h SF media
α-CD3+ α-CD46
K
IL-1β secretion (normalized to ctrls)
HD1-4
P1-7
L
Naive
Memory
Cell populations (%)
HD5 HD6 HD7 P8 P9 P10 P11 P12 P13 P14
M
Spearman r = 0.74
p = 0.03
IL-1β (pg/ml)
Active caspase-1 (%)

Fig. S3

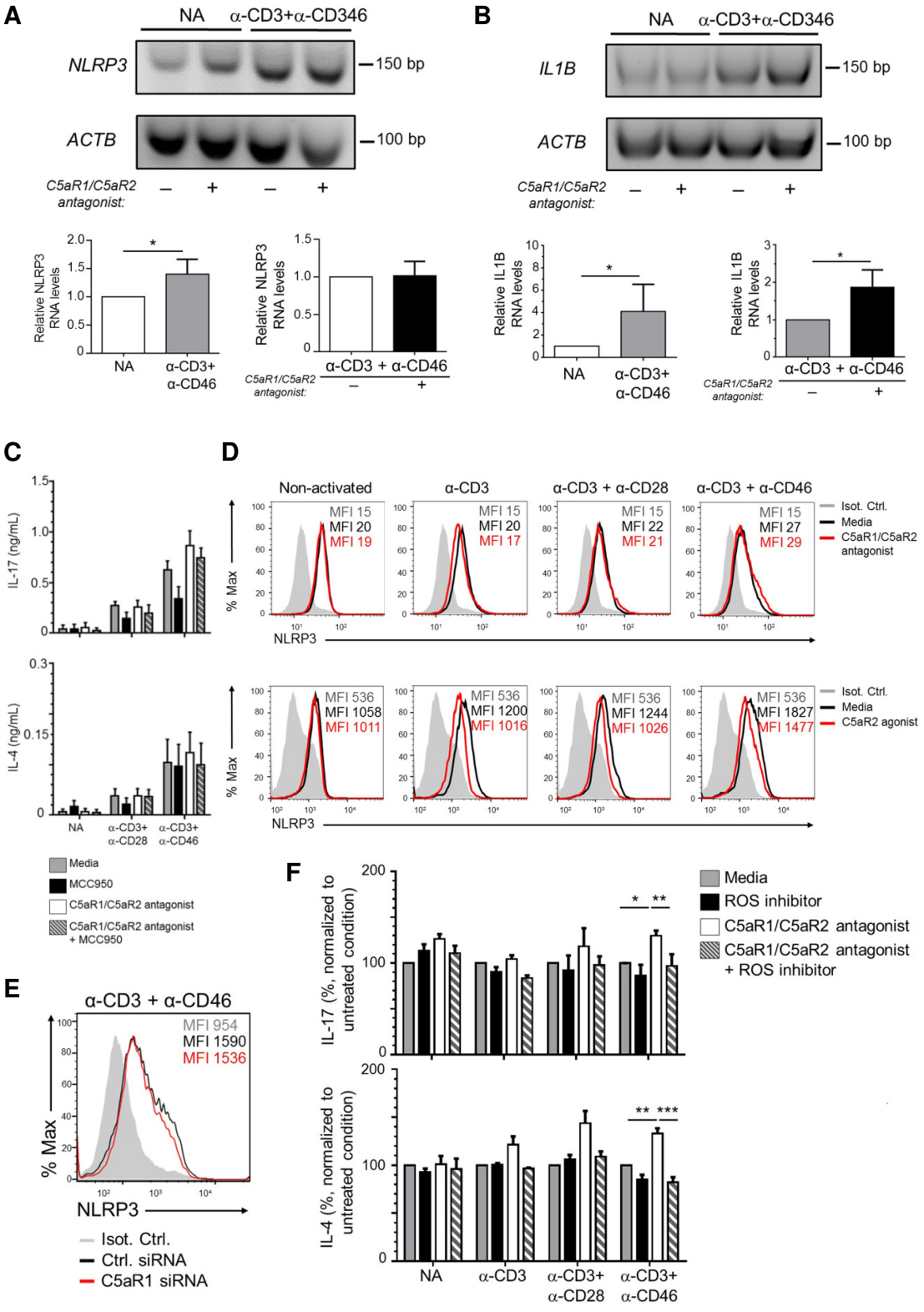
A
NA
α-CD3+α-CD346
NLRP3
150 bp
ACTB
100 bp
C5aR1/C5aR2 antagonist:
Relative NLRP3 RNA levels
NA
α-CD3+ α-CD46
α-CD3 + α-CD46
B
IL1B
Relative IL1B RNA levels
C
IL-17 (ng/mL)
IL-4 (ng/mL)
NA
α-CD3+ α-CD28
α-CD3+ α-CD46
Media
MCC950
C5aR1/C5aR2 antagonist
C5aR1/C5aR2 antagonist + MCC950
D
Non-activated
α-CD3
α-CD3 + α-CD28
α-CD3 + α-CD46
% Max
NLRP3
MFI 15
MFI 20
MFI 19
MFI 17
MFI 22
MFI 21
MFI 27
MFI 29
Isot. Ctrl.
Media
C5aR1/C5aR2 antagonist
MFI 536
MFI 1058
MFI 1011
MFI 1200
MFI 1016
MFI 1244
MFI 1026
MFI 1827
MFI 1477
C5aR2 agonist
E
α-CD3 + α-CD46
MFI 954
MFI 1590
MFI 1536
Isot. Ctrl.
Ctrl. siRNA
C5aR1 siRNA
F
IL-17 (%, normalized to untreated condition)
IL-4 (%, normalized to untreated condition)
Media
ROS inhibitor
C5aR1/C5aR2 antagonist
C5aR1/C5aR2 antagonist + ROS inhibitor
NA
α-CD3
α-CD3+ α-CD28
α-CD3+ α-CD46

Fig. S4

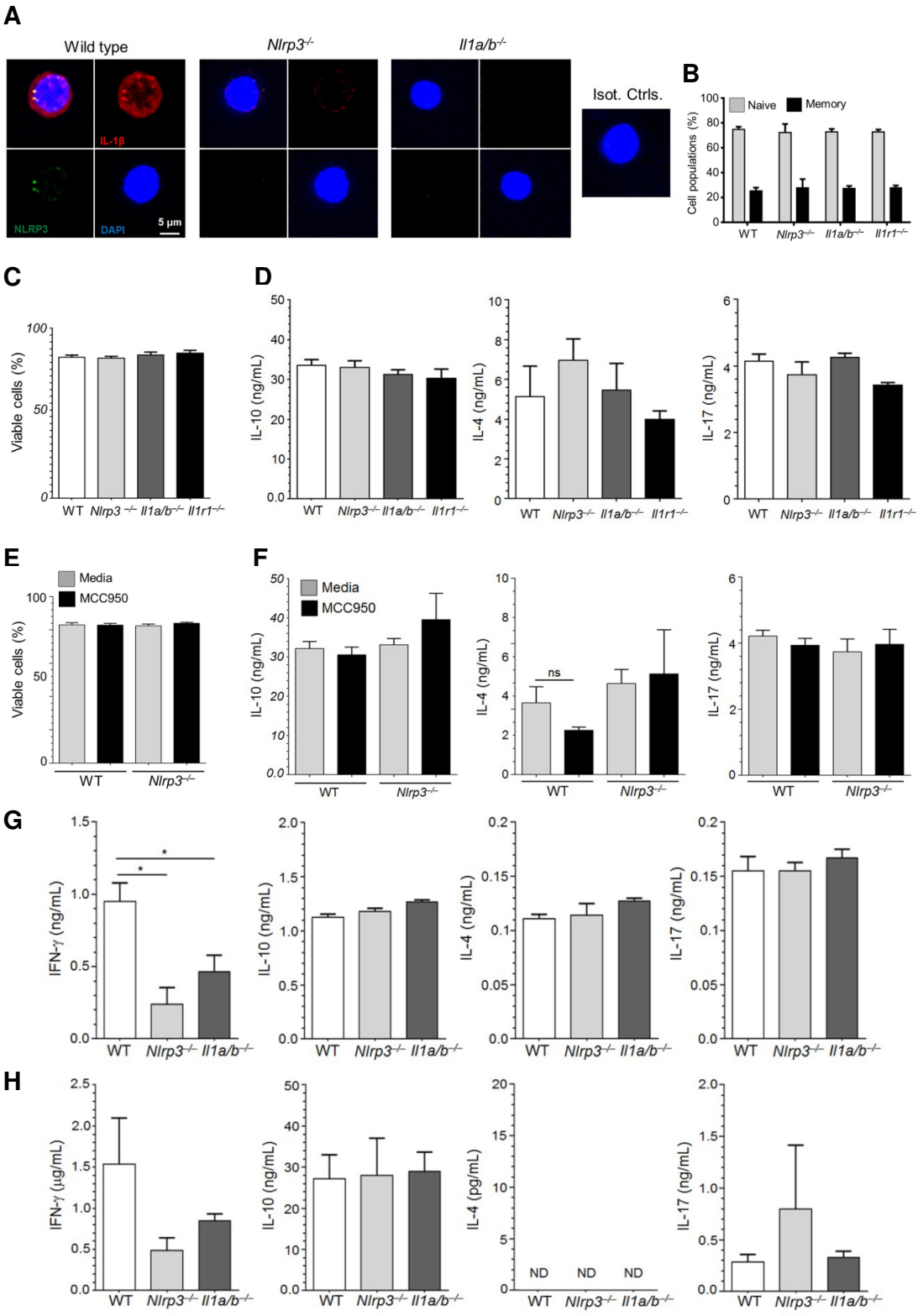
A
Wild type
Nlrp3-/-
Il1a/b-/-
Isot. Ctrls.
IL-1β
NLRP3
DAPI
5 µm
B
Naive
Memory
Cell populations (%)
WT
Nlrp3-/-
Il1a/b-/-
Il1r1-/-
C
Viable cells (%)
D
IL-10 (ng/mL)
IL-4 (ng/mL)
IL-17 (ng/mL)
E
Media
MCC950
F
ns
G
IFN-γ (ng/mL)
H
IFN-γ (µg/mL)
IL-4 (pg/mL)
ND

Fig. S5

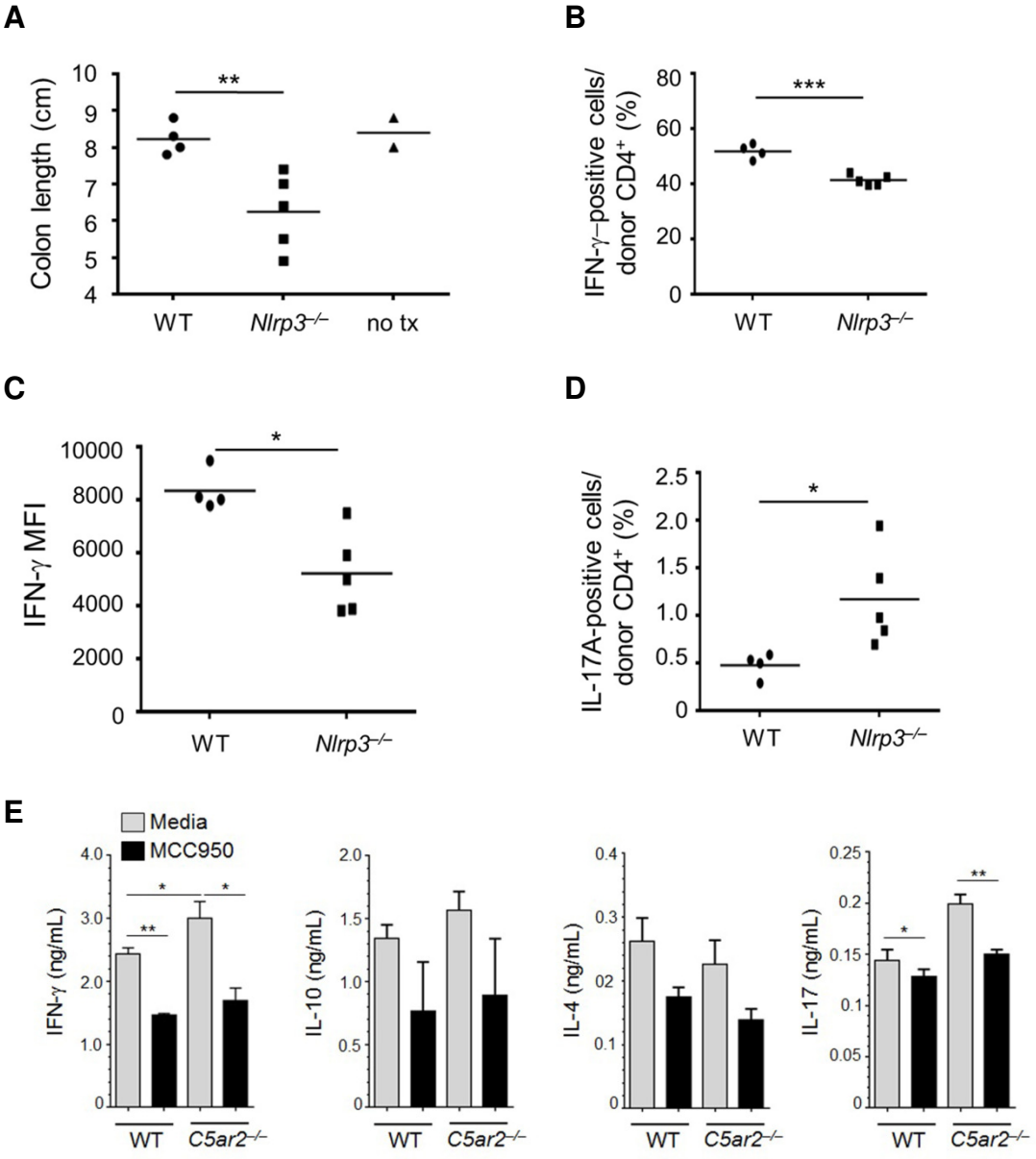
A
Colon length (cm)
10
9
8
7
6
5
4
**
WT
Nlrp3−/−
no tx
B
IFN-γ–positive cells/ donor CD4+ (%)
80
60
40
20
0
***
WT
Nlrp3−/−
C
IFN-γ MFI
10000
8000
6000
4000
2000
0
*
WT
Nlrp3−/−
D
IL-17A-positive cells/ donor CD4+ (%)
2.5
2.0
1.5
1.0
0.5
0
*
WT
Nlrp3−/−
E
Media
MCC950
IFN-γ (ng/mL)
4.0
3.0
2.0
1.0
0
*
*
**
WT
C5ar2−/−
IL-10 (ng/mL)
2.0
1.5
1.0
0.5
0
WT
C5ar2−/−
IL-4 (ng/mL)
0.4
0.3
02
0.1
0
WT
C5ar2−/−
IL-17 (ng/mL)
0.25
0.2
0.15
0.1
0.05
0
*
**
WT
C5ar2−/−

Fig. S6

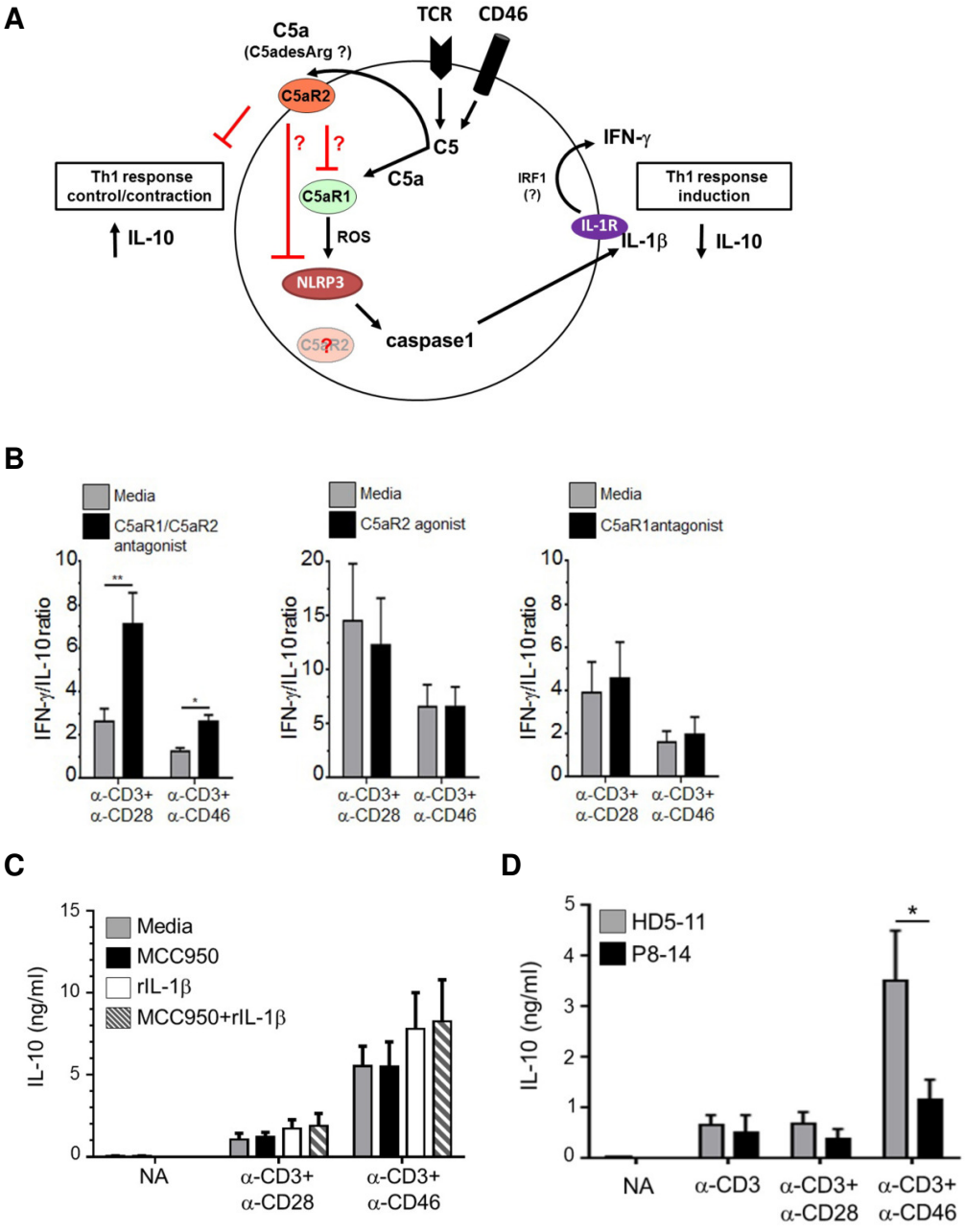
A
C5a
(C5adesArg ?)
TCR
CD46
C5aR2
C5
C5a
C5aR1
ROS
NLRP3
caspase1
C5?R2
IFN-γ
IRF1
(?)
IL-1R
IL-1β
IL-10
Th1 response
control/contraction
IL-10
Th1 response
induction
B
Media
C5aR1/C5aR2
antagonist
IFN-γ/IL-10 ratio
α-CD3+
α-CD28
α-CD3+
α-CD46
Media
C5aR2 agonist
Media
C5aR1antagonist
C
Media
MCC950
rIL-1β
MCC950+rIL-1β
IL-10 (ng/ml)
NA
α-CD3+
α-CD28
α-CD3+
α-CD46
D
HD5-11
P8-14
IL-10 (ng/ml)
NA
α-CD3
α-CD3+
α-CD28
α-CD3+
α-CD46